

Estimating erosion, sediment yield, and dam lifetime using revised universal soil loss equation and potential erosion model in the Chichaoua watershed and Boulaouane Dam, High Atlas, Morocco

Abdeslam Baiddah¹, Samira Krimissa¹, Mustapha Namous^{1,4}, Hasna Eloudi²,
Maryem Ismaili^{1*}, Sonia Hajji¹, Fatima Aboutaib¹, Nasem Badreldin³

¹ Data Science for Sustainable Earth Laboratory (Data4Earth), Sultan Moulay Slimane University, Mghila B.P. 592, Beni Mellal 23000, Morocco

² Faculté des Arts et des Sciences (FAFS), Université de Saint-Boniface, 200, Avenue de la Cathédrale, Winnipeg, MB R2H 0H7, Canada

³ Applied Geology and Geoenvironment Laboratory, Faculty of Sciences, Ibn Zohr University, Agadir 80000, Morocco

⁴ Department of Soil Science, University of Manitoba, 13 Freedman Crescent, Winnipeg, MB R3T 2N2, Canada

* Corresponding author's e-mail: maryem.ismaili@usms.ma

ABSTRACT

Soil erosion is a global challenge with significant environmental, social, and economic impacts. This study, conducted in the Chichaoua watershed, aims to quantify soil loss, investigate its causes, and evaluate its effects on the construction of the new Boulaouane dam. Two models were used to quantify potential soil losses: the Revised Universal Soil Loss Equation (RUSLE) and the potential erosion model (PEM). The results indicate an average annual loss of 10.03 t/ha/yr according to RUSLE, while the EPM provides a higher estimate of 27.53 t/ha/yr. These values, exceeding the tolerance threshold, indicate that the watershed substantially contributes to the downstream sediment load, which could impact the hydrological performance and lifespan of the Boulaouane dam. Furthermore, the spatial distribution of soil losses within the Chichaoua watershed is not homogeneous, a heterogeneity that can be explained by the physical characteristics of the study area. This observation highlights the critical need for implementing erosion control measures, especially in upstream areas. This study reveals the intense erosion impacting the Chichaoua watershed, which presents substantial challenges for the sustainable management of the region's soil and water resources. It underscores the pressing necessity of implementing targeted erosion control strategies, particularly around key infrastructures like the Boulaouane dam.

Keywords: soil erosion, EPM-RUSLE, soil loss, Boulaouane Dam, Chichaoua watershed.

INTRODUCTION

Soil is essential for the balance and preservation of terrestrial ecosystems. It is a natural heritage and a non-renewable resource on a human scale. However, it faces growing threats from natural and human activities that cause its degradation. Water erosion is one of the main factors contributing to soil degradation worldwide (Lammadalena, 2010, Paroissien et al., 2015, Borrelli et al., 2017).

According to the literature, over 10 million hectares of agricultural land are affected by soil erosion every year, with global losses estimated

at around 43 Pg per year (Borrelli, et al., 2020). According to the FAO, 2015, these losses have an estimated economic impact of \$1 billion.

In Morocco, erosion affects 40% of the national territory, with average annual soil losses ranging from 23 to 55 t/ha/year, and extreme values reaching up to 524 t/ha/year in certain areas (Acharki et al., 2022). A significant portion of these soil losses is deposited into reservoirs and dams, diminishing their retention capacity and lifespan. This phenomenon is driven by various factors, including the semi-arid climate, irregular rainfall, rugged or mountainous topography

covering 25% of the national territory, and lithological characteristics that promote particle detachment (El Garouani et al., 2010, KhaliIssa et al., 2016, El Mouatassime et al., 2019).

Various approaches and models have been developed to evaluate soil erosion caused by water. Some rely on surveys and fieldwork, which can be costly, while others are aimed at estimating soil loss or conducting qualitative assessments to identify erosion vulnerability. This variety of methods reflects the complexity of the phenomenon, the numerous contributing factors, and their variability over time and space.

Soil loss quantification models include the physical WEPP (Water Erosion Prediction Project) model by Flanagan and Nearing (1995), the semi-empirical SWAT (Soil and Water Assessment Tools) model proposed by Arnold et al. (1998), and empirical models such as the USLE (Universal Soil Loss Equation) developed by Wischmeier and Smith (1978). The Gavrilovic Erosion Potential Model (EPM) and the Revised Universal Soil Loss Equation (RUSLE) are also widely used tools with universal applicability. The EPM model is particularly effective for evaluating the extent of erosion while generating risk maps (Mosaid et al., 2022).

Meanwhile, the RUSLE model is highly popular due to its simplicity and robustness. It uses a standardized approach at the catchment scale, incorporating topographical, pedological, and climatic factors, along with data on land use and conservation practices. The revised version of RUSLE (Renard et al., 1991) integrates significant improvements based on thorough analyses and an enhanced understanding of erosion processes. These models rely on diverse input data, which often exhibit spatial and temporal variability, making them versatile tools for assessing and managing soil erosion risks.

Most of these models now utilize geospatial technologies, valued for their ability to gather, analyze, and interpret spatial and temporal data essential for estimating soil erosion. In this context, Geographic Information System (GIS) and remote sensing methods are integrated with various erosion models to assess soil loss rates and identify high-risk areas, supporting sustainable land management and soil conservation efforts.

This study aims to develop a database to assess soil erosion risks in the Chichaoua basin using numerical calculations of annual soil losses through the universal empirical models EPM and RUSLE. It also seeks to estimate the volume of sediments eroded and transported within the basin and its

sub-basins, as well as their potential impact on the retention capacity of the future Boulaouane dam.

The results of this study could serve as valuable tools for basin managers to design effective soil and water conservation policies. Their significance would be further enhanced if combined with methods based on field measurements, ensuring the sustainability of future reservoirs.

STUDY AREA

The Chichaoua basin is situated southwest of Marrakech city, between 8°40'0" and 9°0'0" and 31°00'00" and 31°40'00" north latitude, furthest west within the Haouz Mejjate basin, bordered to the east by the Assif Al Mal basin, to the south by the High Atlas Mountains, to the north by the Tensift, and to the west by the Oulad Bousbaa Plain. Covering an area of 2696 km², it is drained by the Oued Chichaoua, the primary waterway in the study area, along with its tributaries, the Oued Imintanout and the Oued Seksaoua. The Chichaoua sub-basin is an integral part of the hydraulic system of the Oued Tensift, which encompasses approximately ten sub-basins (Fig. 1).

In terms of geology, the Chichaoua basin is bordered to the north by Triassic and Jurassic formations, to the east by recent Pleistocene formations, to the west by tributaries of Cretaceous and Tertiary formations, and to the south by Cambrian formations (Fig. 2).

Morphologically, the Chichaoua basin is divided into three distinct zones, the plain area, characterized by an altitude below 800 meters, constitutes a significant agricultural region, accounting for 54% of the total basin area (ABHT.2015) (Tensift Hydraulic Basin Agency). Next is the piedmont area, with altitudes ranging between 800 and 1500 meters. This region encompasses traditional AMH (small and medium hydraulic works) irrigation systems, utilizing surface waters collected by seguias of the Chichaoua Oued. It represents 28% of the basin area. Finally, the mountainous area, with altitudes exceeding 1500 meters, serves as the feeding zone for the Chichaoua watercourse, covering 18% of the basin's territory.

In terms of hydrology, the Chichaoua watershed is drained by the Oued Chichaoua, serving as the collector for the Oueds Ameznass, Imintanout, and Seksaoua, originating in the High Atlas (ABHT., 2013). These three streams are often dry, and their flow is subject to seasonal rainfall variations (Hadri

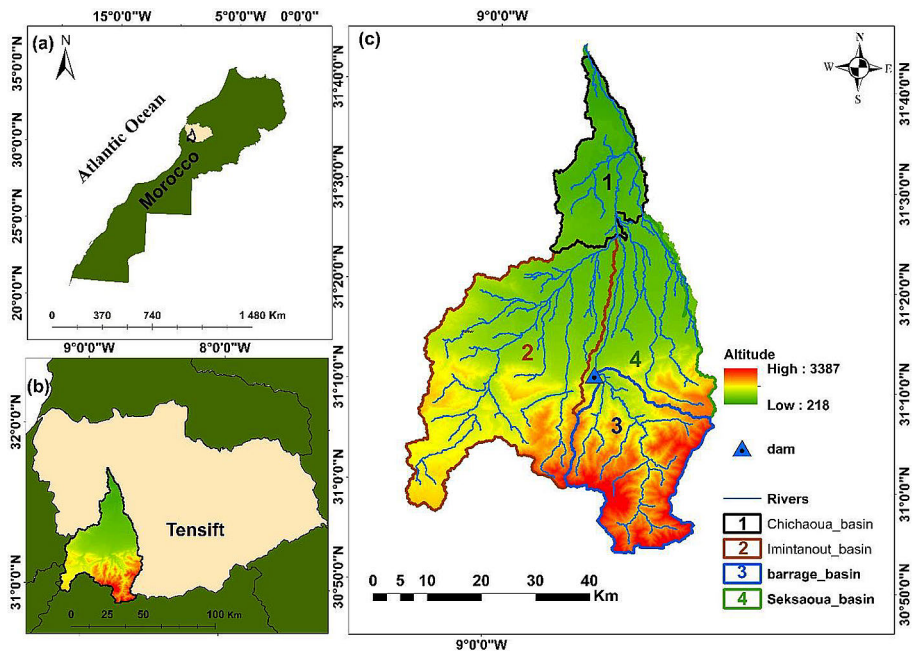


Figure 1. Location maps of the study area (a) at Moroccan scale, (b) at Tensift watershed scale and (c) sub-watersheds of Chichaoua basin

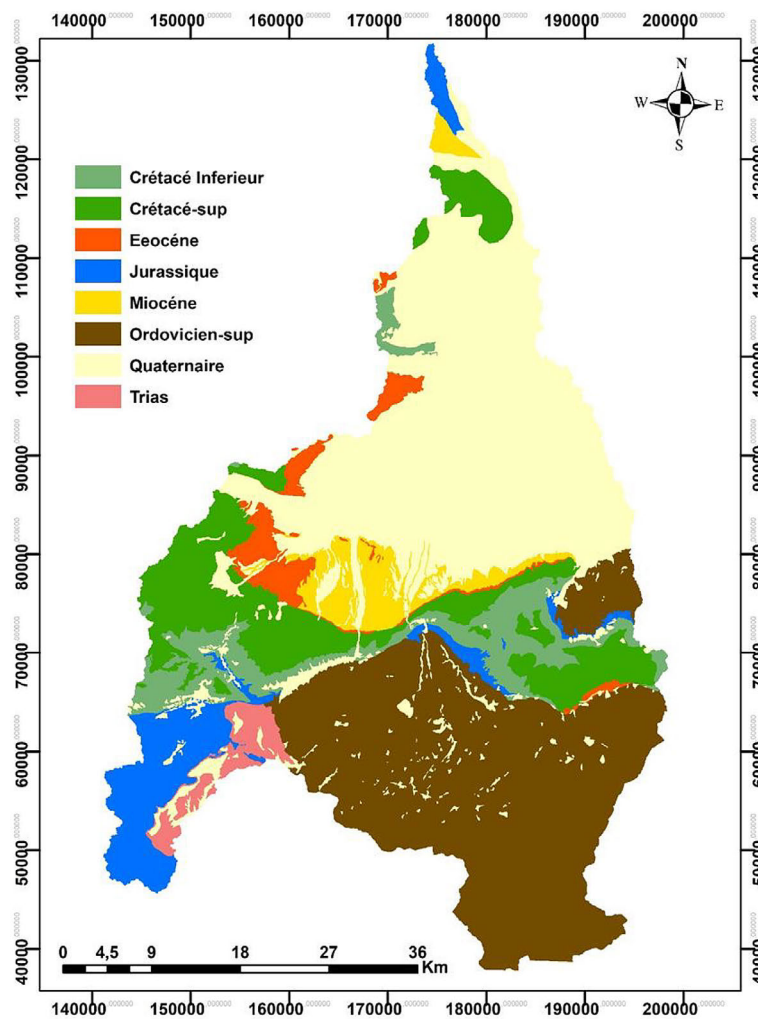


Figure 2. Geological map of the study area

et al., 2021). Additionally, the watershed is equipped with a hydraulic structure, the Boulaouane dam, constructed on the Oued Sekssaoua at the upper sub-basin level (X = 176000, Y = 70000), with a capacity of 66 million cubic meters. This dam is utilized for irrigating the hydro-agricultural perimeter in the Mejjat plain and downstream, as well as for supplying drinking water to the city of Chichaoua and its surrounding areas (PDAIRE, ABHT) (Integrated Water Resource Management Steering Plan).

In terms of climate, the Chichaoua watershed is characterized by low and irregular precipitation, high temperatures, and high evaporation rates, typical of arid and semi-arid climates. These conditions impose significant constraints on agriculture and the water and soil resources of the region. Precipitation gradually increases with altitude from north to south. It is sparse in the plain area (180 mm in Chichaoua) and becomes more abundant as one moves towards the mountains (300 mm in Imintanout and over 450 mm at higher altitudes). The Chichaoua watershed is subdivided into three bioclimatic zones: the dry stage with cold winters covering the entire plain of the basin (54% of the total area), the semi-arid stage encompassing the foothill zone (28% of the basin), and the humid stage, which is less extensive (18%), covering the mountain peaks.

MATERIAL AND METHODS

The methodology chosen for this research study is of paramount importance in understanding and evaluating soil degradation processes through sediment detachment by water erosion. The main objective is to develop a robust and rigorous methodology to estimate these complex phenomena, considering the diverse variables that influence them. This section thoroughly examines the various methodological steps and highlights the models, tools,

techniques, and procedures used to achieve our research objectives (Table 1).

To establish maps of potential soil losses, two models are utilized: the RUSLE model based on Wischmeier’s 1978 equation and the EPM model by Gavrilovic from 1972. These maps are created inside a GIS framework to help compare the two models and anticipate the degree of prospective soil erosion upriver of the Boulaouane dam.

Furthermore, to estimate the lifespan of the Boulaouane dam, currently under construction in the study area, a relationship between the specific degradation of watersheds and the respective annual siltation of dams in Morocco was established based on statistical analyses and data provided by the Hydraulic Basin Agency (Table 2).

RUSLE

The development of the soil loss map, which offers an estimate of erosion in (t/h/year), is illustrated in the accompanying figure (Fig. 3), which depicts the progression of the various steps of the methodological approach of RUSLE.

Wischmeier and Smith 1978 revised the RUSLE equation. The goal was to forecast annual averages of soil loss over a long period of time. RUSLE is made simple to use by a modern computer interface, and it makes use of physically relevant input variables that widely available in databases or can accessed via satellite pictures and DEM (Ganasri et al, 2015).

The original USLE’s structure remained in the RUSLE (Renard et al. 1991, 1994, 1996), but various changes were made to the parameters of the individual equations to account for newly discovered information, data, experiments, and conceptual interpretations of the previously released USLE article.

The RUSLE model is made up of five elements: soil erodibility factor (K-factor), rainfall erosivity

Table 1. Data sources

Data	Source	Descriptions
Rainfall data	ABHT (The Tensift Basin Hydraulic Agency)	Spreadsheet file (average annual rainfall)
Soil type	Soil map of central Morocco	Scale 1/50000
Lithology	Geological map of Morocco and Imintanout	Scale 1/1000000, 1/50000,
TP	www.earthexplorer.com	LDST 8 OLI image - Band 10
Digital elevation model www.earthexplorer.com ASTER DEM (30 m)		
NDVI www.earthexplorer.com LDST 8 OLI		

Table 2. Dam used to illustrate how particular degradation and yearly packing are related (data provided by the Hydraulic Basin Agency, Morocco)

Pre-priority basin dams	Surface (km ²)	Retention capacitymm ³	Specific degradation (t/ha/year)	Degradation in (mt/ha)	Annual packaging (mm ³ /year)
Hassan I	1670	254	26	4.34	2.9
Moulay Youssef	1441	175	27.06	3.90	2.6
Oued El Makhazine	1820	772	37.91	6.90	4.6
Idriss I	3680	1173	8.97	3.30	2.2
El Kansera	4540	265	4.63	2.10	1.4
Bine El Ouidane	6400	1300	11.72	7.50	5
Mansour Ed Dahbi	15000	505	4.7	7.05	4.7
Med Ben A Khattabi	780	43	25	1.95	1.3
Lalla Takerkoust	1707	68	4.39	0.75	0.5
Sidi M. B. Abdellah	9800	477	2.6	2.55	1.7
Youssef BenTachfine	3784	303	8.32	3.15	1.43
Aoulouz	4500	100	3.2	1.44	2.1
Al Massira	28500	2747	1.32	3.76	2.5
Hassan Eddakhil	4400	343	3.99	1.76	1.17
Ibn Batouta	178	36	47.19	0.84	0.56
Nakhla	107	6	42.06	0.45	0.3
Abdelmoumen	1300	213	2.65	0.34	0.23
Hachef	220	300	26.5	0.58	0.5
Melleh	1800	8	0	0.00	0.15

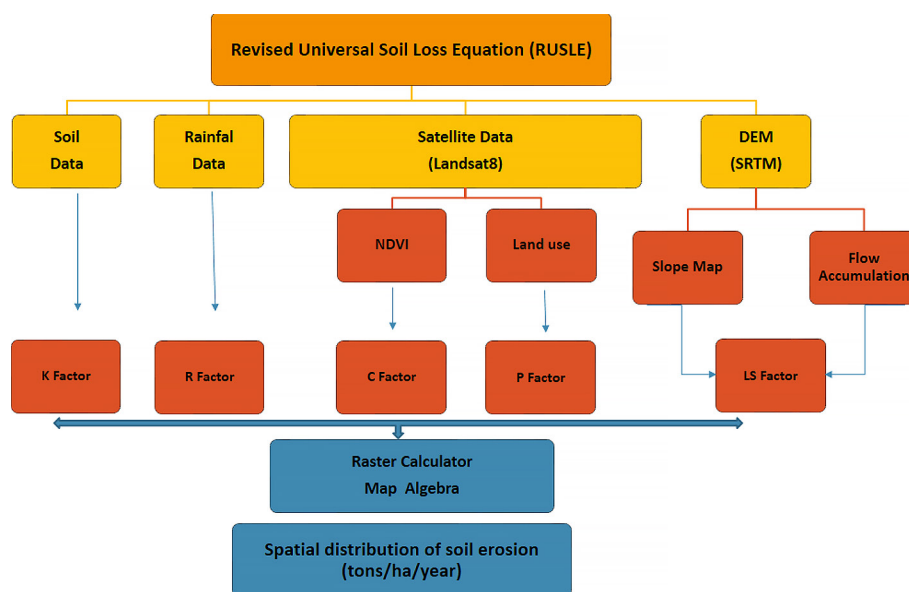


Figure 3. Flow chart of the RUSLE method

factor, (R-factor), slope length factor (LS factor), cover-management factor, and conservation practices factor (P-factor) (Bouamrane et al., 2021).

The utmost intricate component of the RUSLE, the LS-factor, is found by field quantities at the plot scale and is engendered from DEM at the watershed and regional sizes (Zhang et al., 2022).

The RUSLE was utilized in this research study to calculate the soil erosion modulus in the Chichaoua watershed. RUSLE formula is as follows:

$$A = R \times K \times LS \times C \times P \quad (1)$$

The K-factor (t/h/MJ⁻¹/mm⁻¹), R-factor (MJ mm/ha⁻¹/h⁻¹/year⁻¹), LS support (or conservation)

practice factor (P), and cover management factor (dimensionless) are all represented by this equation.

Rain erosion factor (R)

Climate impacts erosion in two ways: by detaching (due to rainfall impact and surface, as described by the R factor (Roose et al., 1976). Equation 2 provides an analytical calculation of the parameter for a single storm. The estimation of R_i for a certain period i is obtained via adding the EI 30 harvests of all erosive storm events. The annual value of the index is calculated as the total of all R_i factors estimated throughout a year's time interval (Wischmeier et Smith, 1978):

$$R = E \times \frac{I_{30}}{1700} \quad (2)$$

$$E = 1.213 + 0.89 \log(I) \quad (3)$$

The only information on precipitation available for resorts in or close to the basin is monthly and annual averages, which has always made this method challenging. The approach suggested by the current study is suitable for this purpose (Renard et al, 1997)

$$R = 0.0483 \times P^{1.61} \quad (4)$$

where: R – climate forcefulness index in $Mjmm/ha/H/year$, P – maximum 24-hour precipitation in mm

With the knowledge of the average annual rainfall, this method estimates the erosion of Wischmeier rainfall R in an indirect manner.

Due to a lack of these data in Morocco, Arnoldus presented a modified method based on Moroccan conditions that uses just average once-a-month and yearly rainfall to estimate the R factor. The data used in this study is from the ABHT (Tensift Hydraulic Basin Agency). Monthly and annual rainfall monitoring began in 1971 and will continue until 2023 at the foremost sites in Chichaoua, Iloujdane, Sidi Bouathmane, and Abadla. This decision is based on the monthly rainfall data available at rainfall stations in the Chichaoua basin. The R factor is expressed as follows:

$$R = 0.26 \times MFI^{1.5} \quad (5)$$

$$MFI = \sum_{i=1}^{12} \frac{p_i \times p_i}{p_i} \quad (6)$$

where: P_i – represents less once-a-month rainfall in mm, while P – represents yearly rainfall in mm. R – values are synthesized from the specialized rainfall data at the scale of Chichaoua watershed.

Soil erodability factor (K)

The soil erodability can be approached in various ways, the simplest of which is the calculation of the soil by employing the triangle (Brown, 2003) (Figure 2) and Stone and Hilborn correspondence (Table 3). This approximate method is based on the development of a link between soil texture and K factor (Stone and Hilborn, 2000). However, it leverages the limitations imposed by the study area to its advantage.

The K factor was predictable by analyzing the mobile surface of each homogeneous unit and to limit the influence of other factors, the average of three to four K values for each lithological formation was taken. It is partial by the soil's structure, texture, granulometry, organic matter content, and permeability (Table 3). The soil erodability factor (K) was calculated using the Wischmeier monogram, along with data from the pediatric profiles of Sabir et al. (2002) and Mandimou (2002), as well as the soil types of Morocco. The erodability values vary from 0.2 ($t/ha/ha^{-1}/MJ^{-1}/mm^{-1}$) on Calcaromagnisimorphe soils to 0.46 ($th/ha/1MJ^{-1}, mm^{-1}$), on soils with low erosion with inclusion of iron sesquioxide soils (Fathallah et al., 2021).

$$K = \frac{(2.1M^{1.4} \cdot 10^{-4}(12-MO) + 3.25(P-2) + 2.5(S-3))}{100} \quad (7)$$

where: K – represents soil erodability (tonnes/ha); MO – the soil's organic matter content; M – it's the result of multiplying the primary particle fractions and is calculated as follows:

$$M = (\%Lemon + \%fine\ sand) \times (100\% \text{ clay}) \quad (8)$$

S – the structural code; estimates from the table established by Wischmeier (1978),

P – the permeability code estimates from the table established by Rawls and all (1982).

Sixteen samples were collected and analyzed in the laboratory. The location of the samples is shown in Figure 4. The sampling and observation sites were selected based on the homogenous unit map, which integrates the geological, vegetation cover, and pedological maps. Each homogeneous unit was assigned the corresponding K value.

Topographic factor (LS)

According to Mahmood et al. (2023), the LS signifies the topographical influence on soil erosion, taking into account both slope length and

Table 3. K-factor parameter estimation several soil types in Chichaoua watershed

Samples	Type of lithofacies	Soil type	P code	S code	% sand	% loam	% clay	% M.O	Texture	K
TRIM	Red pelite and sandstone	RBS	5	1	5.5	65	29	0.5	silty clay loam	0.36
JUIM	Dolomite limestone	CMM-U	2	2	41.3	44.5	11	3.13	loam	0.2
CRFIM	Calcarey, dolomite, limestone, marly	LEL	2	2	27.3	51.7	20	0.64	silt loam	0.25
MIOIM	Sandy clay, marls and conglomerates	SLEE-SIS	2	2	30	20	55	0.8	clay loam	0.25
EOIM	Sandy clay, marls and conglomerates	ISI-C	5	1	13.5	62.2	21.3	2	silty clay loam	0.3
CRSSK	Sandy marl, limestone, phosphates	ISI-CS	5	1	3.04	63.75	30	2.87	silt clay loam	0.3
QCH	Recent alluvium-silt	ISI-CS	6	2	25.3	55	18	1.4	silt loam	0.46
ORSK	Shale, sandstone shale	LDE-RM	1	3	59.5	32.5	5	2.6	sandy loam	0.28

Note: *Red-brown soil (RBS); Calcarmagnismorphic and underdeveloped (CMM-U); Little evolved and lithosol (LEL); Soils Little evolved erosion with inclusion of soils with iron sesquioxide (SLEE-SIS); Isohumic soils with inclusion of calsimagnisic soils (ISI-C); Isohumic soils with inclusion of calsimagnisic soils (ISI-CS); Soils little evolved erosion with inclusion of soils with iron sesquioxide (ISI-CS); Little development in erosions of raw minireux (LDE-RM) (Fig. 5).

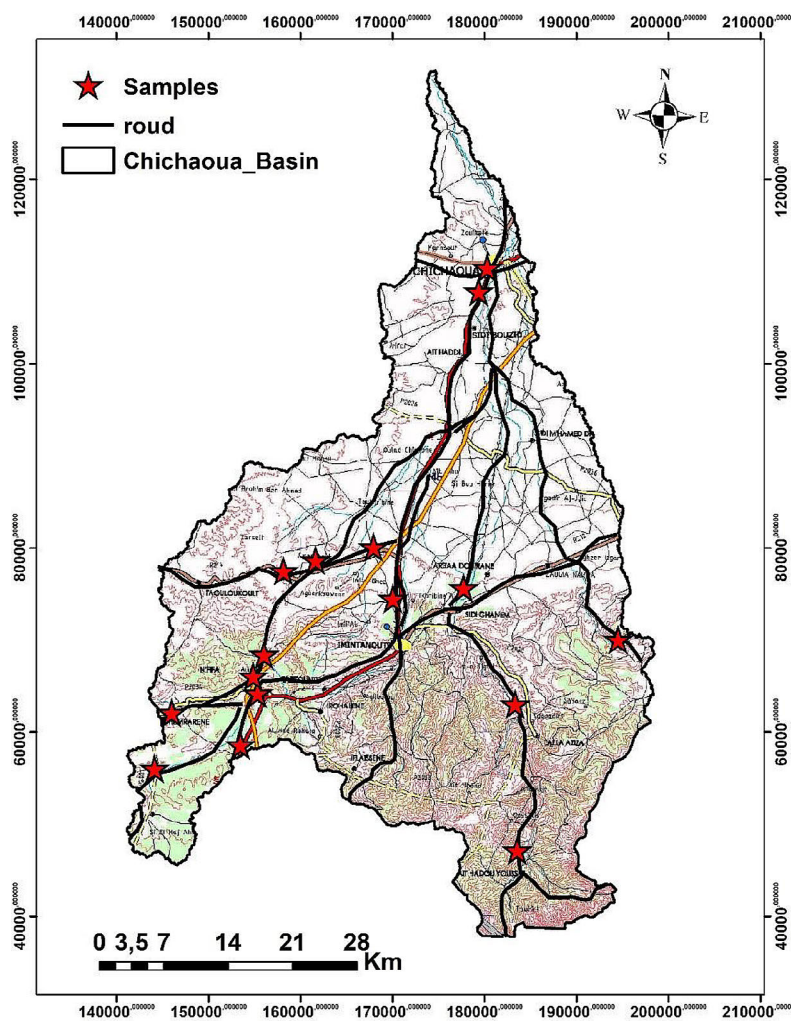


Figure 4. Location of the samples

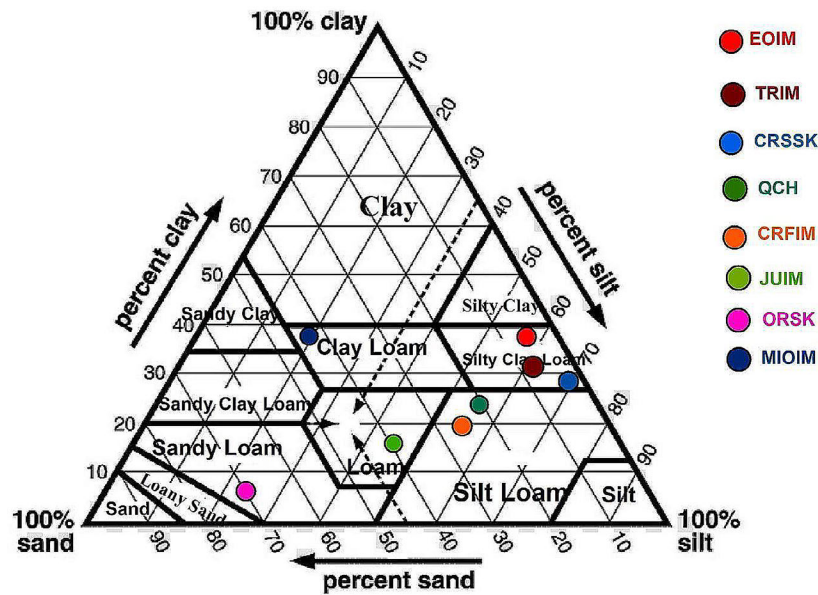


Figure 5. The soil texture triangle (USDA division, 108(2), 166–171)

steepness, which can amplify the properties of rainfall. The slope degree and flow accumulation ascertained from the 12.5-meter resolution DEM (USGS Earth Explore) are included in the LS factor. Equation 9 (Moore et al., 1992), was used to determine the LS.

$$LS = (0.4 + 1) \times \left(\frac{Folowaccumulation \times Cellsize}{22.3} \right)^{0.4} \times \left(\frac{\sin(Slope)}{0.0896} \right)^{1.3} \quad (9)$$

Cover management factor (C)

Among the most significant contributing variables to water, erosion is soil occupation, or surface condition. Its lowering effect varies in a ratio of 0 to 1 on the sediments' detachability (splash) and transportability (scratch). Indeed, values about 0.01 for dense plant coverings to the ground (multi-layer) to nearly 1 for bare soils are taken by the coefficient C of the Wischmeier formula (Wischmaier and Smith, 1981, Bou-imajjane et al., 2020). A land cover map must be created using information from satellite images (sentinel 12.5 m), and fieldwork to assess the diverse vegetation cover units across the Chichaoua watershed.

Using red and near-infrared wavebands, the NDVI was extracted from Landsat-8 satellite pictures, and the C factor was computed using the equation that follows (Durigon et al., 2014):

$$C = 0.1 \times \left(\frac{-NDVI + 1}{2} \right) \quad (10)$$

Support practice factor (P)

The outcome of maintenance efforts is represented by the cultural practice factor P. Crops grown on level curves, alternating terraces or strips, banquet reforestation, buttering, and bullshitting are the best methods for conserving soil (Salma et al., 2023). Land that doesn't apply any of the aforementioned practices is given a value of 1 (Shin, 2008).

The estimation of this element is predicated on the correlation between agricultural techniques and slope (Table 4) (Bou and Belfoul, 2020). It varies based on the modifications that are done. (El Hafid et al., 2017).

Erosion potential model (EPM)

The process of developing the soil loss map, which provides an estimate of erosion in (m³/km²/year), is shown in the accompanying Figure 6, which illustrates the progression of the

Table 4. Value of the factor associated with anti-erosive practices affording to the slope (Shin, 1999)

Slope (%)	P
0.0–7.0	0.55
7.0–11.3	0.60
11.3–17.6	0.80
26.8	0.90
> 26.8	1.00

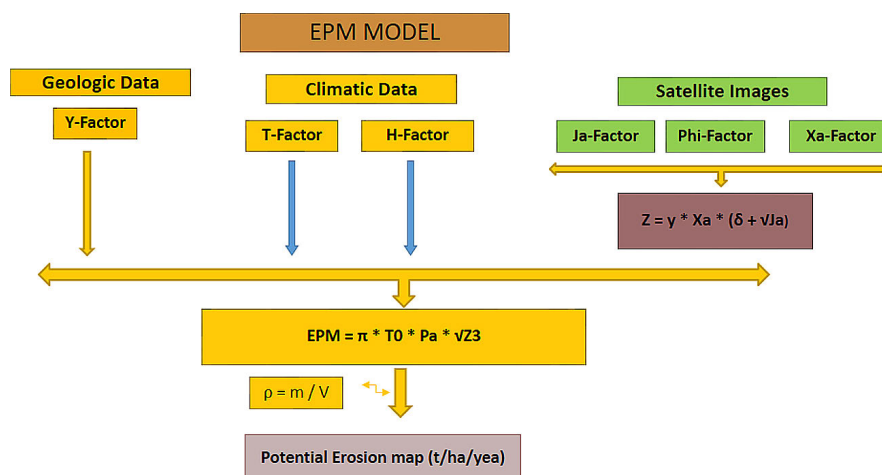


Figure 6. Methodological approach of EPM method

different steps of the methodological approach of the EPM model of Gavrilovic and Smith.

EPM, developed by Gavrilovic (1972), is conditioned estimate probable annual soil losses and assess the spatial vulnerability to erosion. This model incorporates four key factors: lithological, topographical, climatic (AP and Ts), and anthropogenic factors, primarily land use and land cover. The potential soil loss values (W) are expressed in m³/km²/year and are calculated using the following equations:

$$W = \pi \times T \times H \times \sqrt{Z^3} \times F \quad (11)$$

where: *W* is the average annual sediment production (m³/km²/year); *W* – mean annual soil erosion (m³/km²/year); *T* – annual temperature coefficient (°C), calculated from Landsat 8 using the following equations:

$$T = (0.1 \times t_0) + 0.1 \quad (12)$$

where: *t*₀ – average annual temperature in °C; *H* – mean annual precipitation (mm), derived from the interpolation of TRMM precipitation data; *F* – catchment area in km²; *Z* – coefficient of potential erosion.

According to (Hssaine, 2014). the erosion coefficient (*Z*) represents the power of erosion processes. is computed by means of Equation 13.

$$Z = X_a \times Y \times (\phi + \sqrt{J_a}) \quad (13)$$

where: *X*_a – LU coefficient; Φ – measures the observed erosion process; *J*_a – slope (%); *Y* – soil erodability coefficient.

The (*X*_a) is determined using NDVI proposed by Gavrilovic, (1972).

Soil erodibility coefficient (Y)

The soil sensitivity coefficient (*Y*), similar to the *K* factor in RUSLE equation, is founded on data regarding OM, soil structure, and permeability. The soil sensitivity map (Fig. 6d) reveals that the matter Chichaoua basin is predominantly covered by land highly sensitive to erosion. This is consistent with land use data, which shows that the basin is mainly composed of rocky and bare terrain, conditions that exacerbate the erosion process.

Soil protection coefficient (Xa)

An area’s capacity to prevent erosion is resolute by two key factors: the coefficients of plant cover and land use. This combined factor is known as the coefficient of soil protection. Both factors are evaluated as a single determinant when assessing soil protection (Hembram, et al., 2019).

The Chichaoua catchment’s *X*_a parameter was determined using Equation 14 as follows:

$$X_a = X_aNDVI - 0.61) \times (-1.15) \quad (14)$$

Table 5. Values of the *X*_a coefficient’s EPM coefficient (Gavrilovic, 1972; Lazarevic]

Coefficient of soil cover	Xa factor
Mixed and dense forest, thin forest with grove	0.05–0.20
Coniferous forest with little grove, scarce, bushes, bushy prairie	0.20–0.40
Damaged forest and bushes, pasture	0.40–0.60
Damaged pasture and cultivated land	0.60–0.80
Areas without vegetal cover	0.80–1.00

The EPM guide’s table (Gavrilovic, 1972; Lazarevic, 1985) is then used to calculate the Xa value. It results in five classes of Xa coefficients (Table 5). The classes range from 0.1 for highly densely covered areas in flora to 1 for badlands.

Average slope of the study area (Ja)

The slope’s degree of inclination affects the extent of erosion. Numerous research has proven this. (Chaaouan et al., 2022). A rise in slope amplifies runoff, making it more prone to erosion and more energetic than rainfall (Jain et al., 2010; Mohammed et al., 2020).

The topography-derived slope inclination is thought to be the primary component that increases soil sensitivity when rainfall occurs. Growing slopes cause the flow velocity to rise, which influences the creation and movement of more sediment into the watershed (ROOSE., 1994). The DEM (digital elevation model) was used.

Coefficient of type and extent of erosion (φ)

The φ factor reflects the degree of severity of the erosive processes occurring in a given area. This coefficient is calculated according to Equation 15.

The φ factor represents the intensity of erosive processes occurring in a specific area. This coefficient is determined using the following Equation 15.

$$\Phi = \frac{\sqrt{R}}{Q_{\max}} \tag{15}$$

In this context, R represents the B4 when using Landsat 8 images. Q_{\max} is the value gotten from the associated MTL file of the Landsat8 (quantizee_cal_max_band_4=65.585).The φ coefficient values range from 0.1 to 1. Affording to Gavrilovic and Lazarevic, a reference Table 6 is provided to establish the relationship among the calculated values and the severity of erosive processes.

RESULTS AND DISCUSSION

Given its permanent harm to soil and water supplies, soil degradation is considered a problem that affects both people and property. Additionally, by identifying regions susceptible to soil erosion a crucial first step toward sustainable management – the identification of sub-basin’s like naturally occurring units About soil loss research helps supervisors put management of soil erosion approaches into practice.

According to the several field missions, the catchment region of Chichaoua exhibits four different forms of erosion. These areas, which are primarily located in the basin area’s south-east south-west regions and, are characterized by a strong slope and friable materials that have been stripped of vegetation. In this area of the basin, gullies are frequently eroded; they are mostly found in tertiary deposits, clays, and friable Neogene phosphate marl. The remainder of the study region has little erosion. These are mostly composed of outcrops of rock that are extremely able to tolerate erosion; they also contain plain area having a very slight incline and terrain that is shielded by a sizable amount of vegetation. These regions, which are a significant component of the Hercynian basement, are mostly composed of Quaternary-aged detrital rocks and primary-aged (Cambro-Ordovician) volcanic matrix, schists, graywackes, and limestone bars. In this area of the Chichaoua watershed, sheet erosion and debris floods are frequent occurrences (Baiddah et al. 2023) (Fig. 7).

Implementation of RUSLE model

Loss of soil estimates within the basin of Chichaoua were derived utilizing the RUSLE model. Using a System of Geographic Information (GIS), the model’s various parameters were estimated and mapped. The basin’s erosion risk map is the outcome of these several elements interacting (Fig. 8).

Table 6. φ coefficient [Gavrilovic, Lazarevic]

Coefficient of type and extent of erosion φ	φ factor
Slight erosion on the catchment	0.10–0.20
20–50% of the catchment area has erosion in rivers and streams	0.30–0.50
Erosion in rivers, gullies, and alluvial deposits, karstic erosion	0.60–0.70
50–80% of drainage basin is impacted by surface erosion and landslides	0.80–0.90
Erosion affects entire catchment	0.90–1.00



Figure 7. Different form of soil degradation noticed in the basin of Chichaoua: a) Gully erosion; b) Badland;

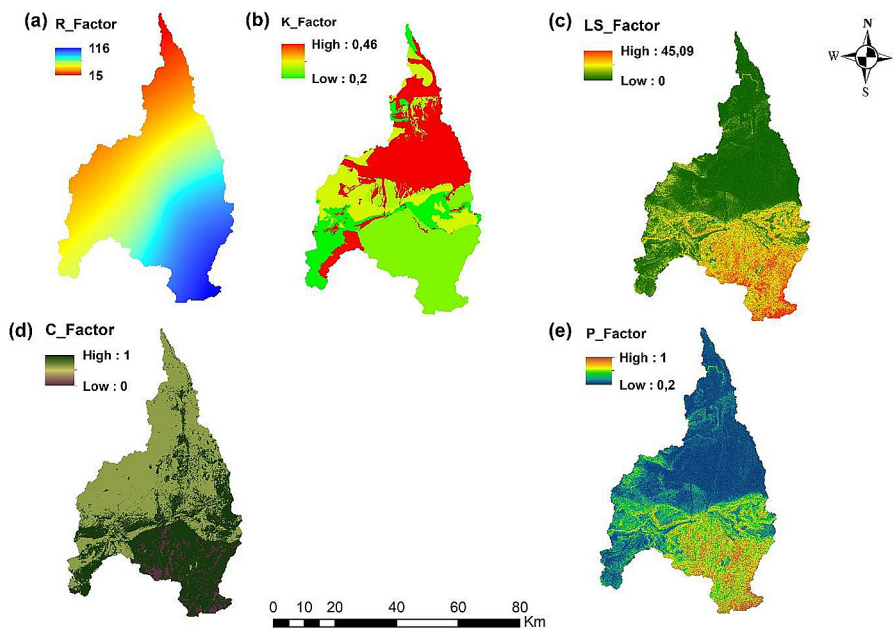


Figure 8. RUSLE model conditioning factors: a) R factor; b) K factor; c) LS factor; d) C factor and e) P factor

Rain erosion factor (R)

The R-factor's spatial distribution across the watershed was displayed in the erosivity map (Fig. 8a). The R factor's values fall within a

variety of 15 to 115 MJ·mm/ha/h an both down-stream and upstream areas within the watershed have modest to moderate values. In contrast, at the level of the basin is high to very high values, and from the northwestern part of the basin

to the southeastern, rain aggression increases. The Chichaoua watershed is exposed to high levels of climate aggression in 55% of cases, as indicated through such a value of R surpassing 50 MJ mm/ha/h/an. Therefore, it may be concluded that rainfall’s erosive strength significantly affects this area.

Soil erodability factor (K)

Three soil classes are identified by the computed K erodability index values, which range from 0.2 to 0.46 (Table 7) on soils of calcarmagnisimorphe and less developed.

Some surfaces show a large amount of rough elements that slow down erosion by intercepting rain drops and reducing the flow speed. For example, in the case of soils little evolved erosion with inclusion of soils with iron sesquioxide and little evolved and Lithosol (Table 3).

Upon assigning a K erodibility value to each soil type, the various soils are classified, and it is found that over half of the soils (59%) have moderate erodibility (0.20–0.30). Vertisols are the least common in the area, with just 6% of the total, and they have a low erodibility (> 0.2), 34, 63% of the studied area is made up of certain highly erodible undeveloped soils (0.30–0.46) (Table 7)

The most erodible terrains are found in the downstream section (the basin’s extreme north) and the southeast section among the sloping watershed, which is home to the Quaternary and triassic erosion-prone covering, according to the erodibility map (Fig. 8b). The soils that make up the great bulk of the pool’s region in the center and southwest regions of the watershed, known as the Calcimagnisque type, have a low to medium erodibility coefficient. Soils

and soils with minimal erosion, somewhat low amounts of organic matter and raw minerals present in coarse sands.

Given that over 50% of the basin has a K index of erosion between 0.20 and 0.30, the soils in the basin are moderately vulnerable to erosion.

Topographic factor (LS)

Five classes have been created from LS values, which range from 0.05 to 45 (Fig. 8c). In the erosion process, the length of the slope and inclination are critical factors.

In the approaching affluent regions of the Chichaoua Watershed, LS values are quite high. 62.32% of the basin area is represented by the LS index that is deemed low, which is between 0 and 5 (Table 8). This is consistent with plains regions, riverbed areas, and low-altitude areas. Because of this, there is a significant chance of erosion throughout the basin from top to bottom. These findings align with the findings of other authors in different basins (Yjjou et al. 2012; Yjjou et al., 2014; Markhi et al., 2015). Research indicates that the rate due to erosion escalates greatly with slope angle, with a mean exposure of 1.4 (Elboukaou et al., 2005). Similar to this, it has been observed whenever the slope increases, the kinetic energy of the rain stays steady as the runoff’s energy kinetics increase, causing the transport to accelerate downward (Ibrahimi et al., 2005).

Plant cover factor (C)

The coverage and level of vegetation cover are represented by the C factor. The high southwest and the southeast area of the Chichaoua basin are primarily covered through low-vegetation

Table 7. Pedological units of the research region and associated K values

Soil erodability class (K)	Vertisols soil type	Area (ha)	Area (%)
Low < 0.2	Vertisols	16140.31	6.37
Moderate (0.20–0.30)	Calcimagnesians, raw minerals, fersiallitic, isohumic and less developed	149272	59
High (0.30–0.46)	less developed	87777	34.63

Table 8. Class of slopes and corresponding surfaces

Slopes	Class (%)	Area (ha)	Area (%)
Low	0–5%	157799,6	62.32
Moderate	5–15%	62586.6	24.72
High	15–20%	20172,5	7.97
Very high	20–45%	12628,51	5

soil occupations, which are the region’s most susceptible to erosion, according to the coverage index’s geographical distribution map (Fig. 8d).

The findings indicate that while about 90% of the basin’s surface has an average to minimal rate of plant cover, 5% of the area has a rate of dense plant cover that is well protected with $C < 0.5$ (Table 9). Asylum voids, clear forests, degraded roads, and farmed land that is thought to be extremely susceptible to erosion are examples of areas with weak vegetation coverage. In (Melihó et al., 2016). Dense forests, dense meadows, and timber cultivation have values less than 0.5. Clear seed and clear matorrals, as well as low density woods, are found in locations with values between 0.5 and 0.9. Bare soils and harvested cereal fields are associated with values that incline towards 1. Water-susceptible areas are those with low plant coverage (C factor greater than 0.5).

Factor of anti-erosive practices P

Effective soil conservation strategies include cultural methods including buttering, billowing,

alternating-band or terrace crops, and level-curved harvesting.

P factor values are either one or less than one. Land devoid of anti-erosive measures has a rating of 1. The slope and the technique of agriculture or management of erosion that is employed both affect the P factor.

It should be mentioned that slope was used in this study to obtain the P factor values (Shin, 1999). Low to moderately sloping areas are represented by medium and low values. P factor values range from 0.2 to 0.25 for places with low slopes and ranging from 0.25 to 1 for regions involving steep slopes. For 43% of the basin’s surface, the value of P equals 1 (Fig. 8e).

Soil loss assessment

Climate aggression is one of the parameters (R) in the RUSLE model, soil erodibility (K), Plant Cover (C), LS, or topographic factor, and anti-erosive methods combine to produce soil losses. The soil loss map at any place in the spill

Table 9. The values of the C factor by soil occupation type

Types of soil occupation	C factor	Area (ha)	Area (%)
Forest	0.04	13195.71	5.22
Feed forests	0.18	133377.84	52.75
Arboriculture	0.28	100579.23	39.78
Naked land, naked landscape	1	5677.29	2.24

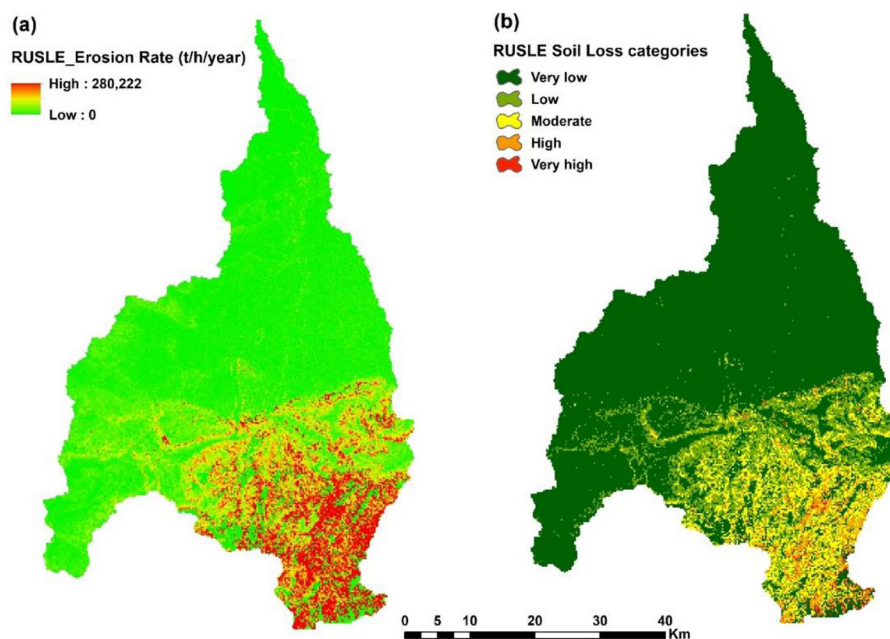


Figure 9. Map of land losses in the Chichaoua basin

Table 10. Chichaoua Basin soil loss distribution

Erosion	Pertes en sol (t/ha/an) S	Area (ha)	Area (%)
Very Low erosion	0–10	184010.22	73.36
Low erosion	10–30	33593.70	13.4
Moderate erosion	30–50	20126.85	8.02
High erosion	50–90	11662.88	4.65
Very high erosion	90–280	1421.15	0.56

basin can be obtained by combining maps of this important variables in a GIS setting (Fig. 9).

Synthetic index produced through multiplication has a mean of 10,03 t/he/year and the range from 0 to 280 t/ha/year (Fig. 9a). Five value classes were created out of the basin’s soil losses (t/ha/year) (Fig. 9b and Table 10). Less than 10 t/ha of land is lost annually in the first class of locations. It mostly encompasses the regions upstream and in the middle of the watershed, making up 73% within the basin’s total region (Fig. 10).

The second category includes regions where land loss occurs at a rate of 10 to 30 t/ha annually. 13% of the basin’s total area is made up of it. The third class includes regions where land loss occurs at a rate of 30 to 50 t/ha annually. 8% of the basin’s total area is made up of it. Areas that lose more than 1000 t/ha annually are included in the fourth class. It makes up only 4 percent of the watershed’s surface. Areas losing more than 100 t/ha annually are included in the fifth class. Merely 0.7% of the watershed’s surface is comprised of it. The last two classifications are associated with regions that are often found near the top of the watershed and are mountainous or have weak substrate.

For instance, the watershed’s surface erosion rate exceeds 50 t/ha annually on 6% of its surface.

This indicates an extremely high rate of erosion that pedogenesis is unable to counteract. These regions, which can be found in the spill basin’s southeast and southwest, have fragile materials, are devoid of flora, and have harsh terrain (60°). Near the groves, where there is flat land with an extremely low incline (5° to 7°) and the density of plants on irrigated land that penetrates in the ground, giving it a high level of erosion resistance, are the main locations of the low losses, which fall less than the ability to tolerate threshold (<7 t/ha/year) and impact 73% among the spilling basin’s surface area.

Most of the southeast region is extremely vulnerable to erosion, especially the region closes to where the future Boulaouane dam will be retained (Fig. 14c). A significant amount of Sediment is produced due to this extreme erosion exposure, which directly contributes to the packing risk. The fact that the eroded sediments only deposit inside the dam indicates how close this location is to the dam, which further adds to the packing.

Implementation of EPM model

Combined with water erosion parameters, such as soil sensitivity, protection, temperature, precipitation, erosion kinds, and slopes (Fig. 11)

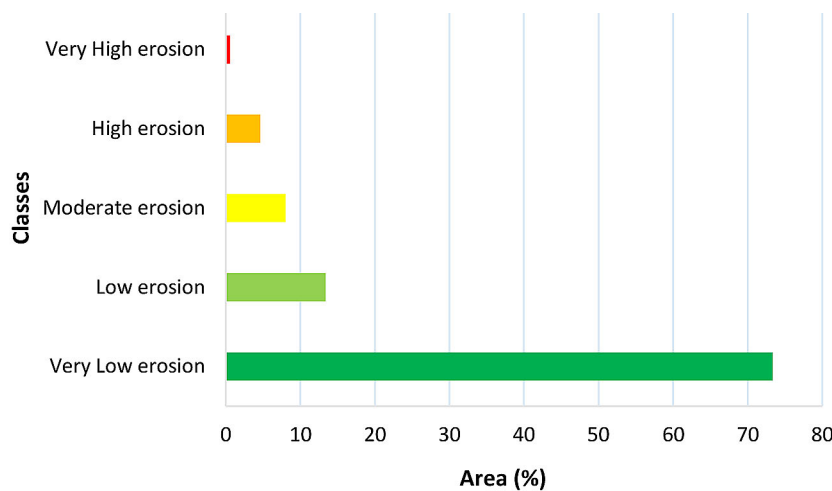


Figure 10. RUSLE classifications of erosion in the Chichaoua watershed

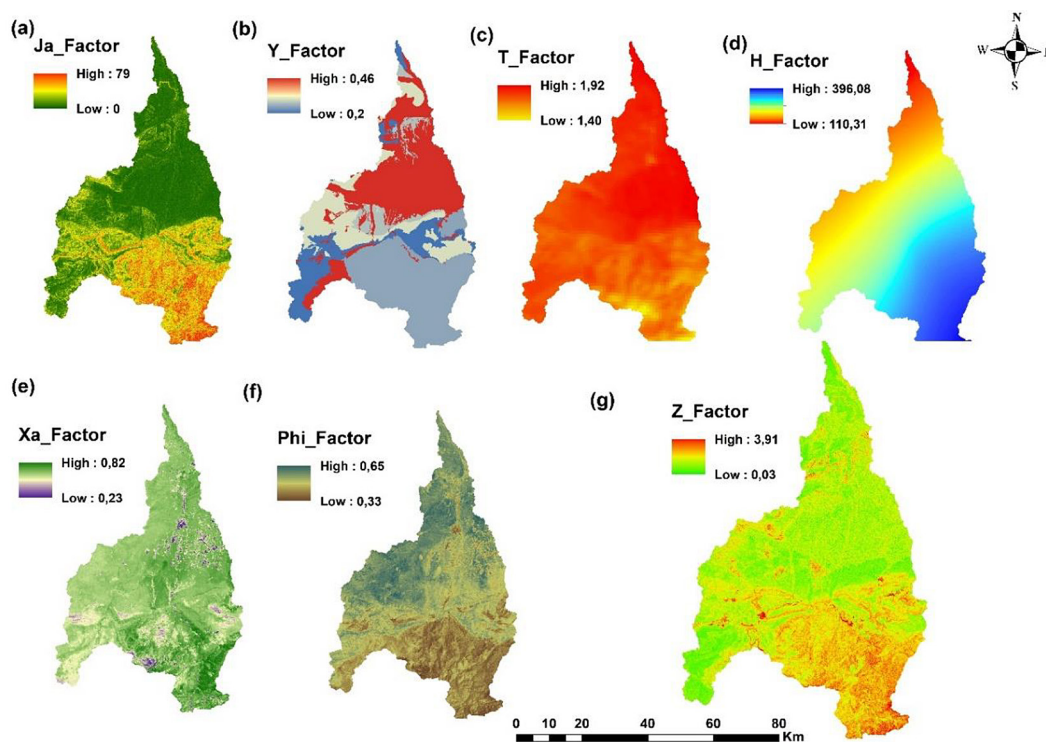


Figure 11. The conditioning elements of the EPM model: a) Ja factor; b) Y factor; c) T factor; d) H factor; e) Xa factor; f) Phi factor; and g) Z factor

forms the basis of the EPM model. Gavrilova’s equations are used to quantify soil losses (Gavrilović, 1972).

GIS software will be used for the modeling of these parameters. We plan to create a map that illustrates the location and impact of every component in the Chichaoua basin. When combined, they will yield an estimate of the area’s potential for erosion. The following six variables are multiplied by erosion in the equation: temperatures, precipitation, slopes, types of erosion, soil protection, and soil susceptibility (Zahnoun et al., 2019).

Slope (Ja)

Erosion is influenced by the incline of the terrain in the Chichaoua basin. Numerous research has proven this (Salma et al., 2023). Lands with low slopes (6%), those with moderate slopes (17%), and those with high and influencing slopes (78%), are often distributed differently (Fig. 11a).

Soil sensitivity (Y)

The K component in Rusle’s equation is comparable to the soil sensitivity coefficient

(Y). Information about soil permeability, structure, and organic matter are also needed. Most of the land in the Chichaoua basin is susceptible to soil erosion at a low to medium level, according to the soil sensitivity map (Fig. 11b). This is entirely consistent with the land occupancy data, which indicates that the vast part of the watershed is made up of bare, rocky terrain, which promotes erosion.

Temperature coefficient (T)

The primary factors influencing soil conditions on a wide scale are temperature, solar radiation, and climate (Mosaid et al., 2022).

When calculating the mean annual temperature (T), the operational land imager (OLI) of Landsat 8’s thermal band 10 is used to measure the temperature of the cloudless surface, clear images from satellites. From 2000 to 2020, this process is run on every picture band for every month. The yearly average temperature in the basin of Chichaoua is found to be generally between 1.39 °C and 1.92 °C when the equation $(0.1 \times \text{temperature}) + 0.1$ is applied. This distribution will be seen by creating the map (Fig. 11c).

Mean annual precipitation (H)

The primary cause of soil erosion is precipitation. Their significance extends to the evaluation of water resources. The challenge facing the Chichaoua basin is addressed in this yearly assessment, which stems from the absence of evenly spaced rain stations on the basin’s surface. Because of this, estimating the dispersion of precipitation in space from the closest rain stations towards the basin is challenging.

To reduce this issue, we have considered the current correlation between yearly precipitation and altitude to estimate precipitation in areas where stations do not exist.

The map derived from this correlation (Fig. 11d) indicates that The south receives the most rainfall each year, in the upper region of the rolling basin, or around 396 mm, while the lowest amount occurs in the northern part of the spilling watershed, at the departing area’s level, with a 110 mm yearly value.

In general, we can state that the bulk of the basin has high rains, with little variation in rainfall. It’s crucial to remember, though, that precipitation is one of the factors in this study that raises the danger of erosion. Elevated precipitation regions are generally more vulnerable to erosion, and vice versa.

Soil protection coefficient (Xa)

Due to its effect on evapotranspiration and infiltration, the soil protection coefficient (Xa) regulates the runoff process (Zahnoun et al., 2020). As a result, it is connected to the plant that gives the soil some support. According to its occupation, the accompanying table (Table 11) displays the level of soil preservation in the watershed of Chichaoua.

Table 11. Soil protection values according to its occupation

Land use	Soil protection Xa	Area (ha)	Area(%)
Groveless coniferous forest with sparse bushes and a bushy prairie	0.2–0.4	446.85	0.17
Destroyed bushes, pasture, and forest	0.4–0.6	33676.74	13.31
Damaged agricultural land and pasture	0.6–0.8	218725.56	86.50
Area without vegetal cover	0.8–1	0.36	0.00014

Table 12. Erosion state coefficient

Type of erosion	Coefficient of the erosive state (Ψ)	Area (ha)	Area (%)
Low and stream erosion	0.2–0.4	3730.95	1.47
Advanced River erosion, Alluvial deposits and ravines	0.4–0.6	247221.9	97.77
landslides and surface erosion	0.6–0.8	1896.66	0.75

The Chichaoua basin’s vegetation distribution is diverse. The amount of plant cover and the soil protection coefficient change simultaneously (Fig. 11e). In contrast to regions with abundant vegetation, damaged pasture and farmed land make up a large portion of the basin and typically provide less ground protection. It offers robust protection for the soil.

The table and figure demonstrated how Xa values range from 0.2 to 1. Minimal values (0–0.4) are observed close to the wadi, indicating the precise locations of dense vegetation. We typically identify high values between 0.6 and 1 in cultivated land, ruined pasture, and areas devoid of vegetation, where protection is lacking.

Coefficient of the erosive state (Φ)

The degree of erosion and the process that caused it are represented by the erosion coefficient Φ, which indicates the erosive state of the basin. Usually, it has a value of 0.1 to 1. It was possible to create a categorization (Table 12) that illustrates the level of dominating erosion for each zone by using field data collection and a basic preliminary analysis of the Chichaoua basin (Fig. 11f).

Estimation of erosion in the watershed of the Chichaoua basin

The combination of the contributing parameters obtained above will allow us to first calculate the erosion coefficient Z (Fig. 11g) and then to estimate the annual soil losses per unit of m³ per km² per year. The result is subsequently converted to t/ha/year so that we can compare it to the Rusle model’s outcomes. Conversion is done by turning kilometers to hectares and also by multiplying the results by the means of the densities attributed to the materials constituting the soil (t/m³). To

calculate Z, we will use data on soil sensitivity, slope, soil protection (Xa), erosive state (Φ) according to the Equation 13.

Soil loss estimation according to Gavrilovic’s EPM model

According to Gavrilovic’s model, the numerous parameters influencing the erosion potential add up to an estimate of the volume of loose soil at each catchment area point. Using this methodology, the quantification of erosion within the basin of Chichaoua led to light the forms and intensity of erosion resulting from the physical, hydrological, meteorological, and topographical aspects of the river basin. Additionally, the yearly transport and sediment yield. As a result, erosion-prone locations were found. The findings demonstrated that the basin is subject to both mild and severe erosion processes, making it possible to identify regions with a higher potential for erosion and others with a lesser potential. This variation can be explained by the separation of elements that govern the natural phenomenon’s

intensity. An estimate of the total average is 27.53 t/ha/year. The annual losses are as follows: 0.13 t/ha at the minimum and 290.21 t/ha at the maximum. To mitigate the consequences and repercussions due to erosion, we might therefore allocate regions with a large yearly output of sediment to regions with a high risk of erosion. Erosion is essentially declining in this area in contrast to other regions where the yearly generation of sediment is still minimal. The higher soil loss rate in the area can be accounted for by an overestimation of the sediment yields from all forms of erosion (Fig. 12a)

The Southeast portion of the watershed, close to the Boulaouane dam, accounts for 16% of the watershed’s high and extremely high land losses, which exceed 80 t/ha/year. It suggests that the phenomenon is spreading slightly. 18% of the entire study area has losses which vary between 30 and 50 t/ha/year., in contrast, most of the studied area (66%) is covered by the low to very low intensity class (less than 30 t/ha/year in soil losses), that is concentrated in the basin’s north and south-central regions. With the objective to lessen

Table 13. Degrees of erosion on the Chichaoua basin’s surfaces

Erosion	Classes of the annual eroded soil (t/ha/year)	Area (ha)	Area (%)
Very low erosion	0–15	83270.43	32.94
Low erosion	15–30	82678.32	32.70
Moderate erosion	30–50	45014.58	17.80
High erosion	50–80	34570.89	13.67
Very high erosion	80–290	7287.48	2.88

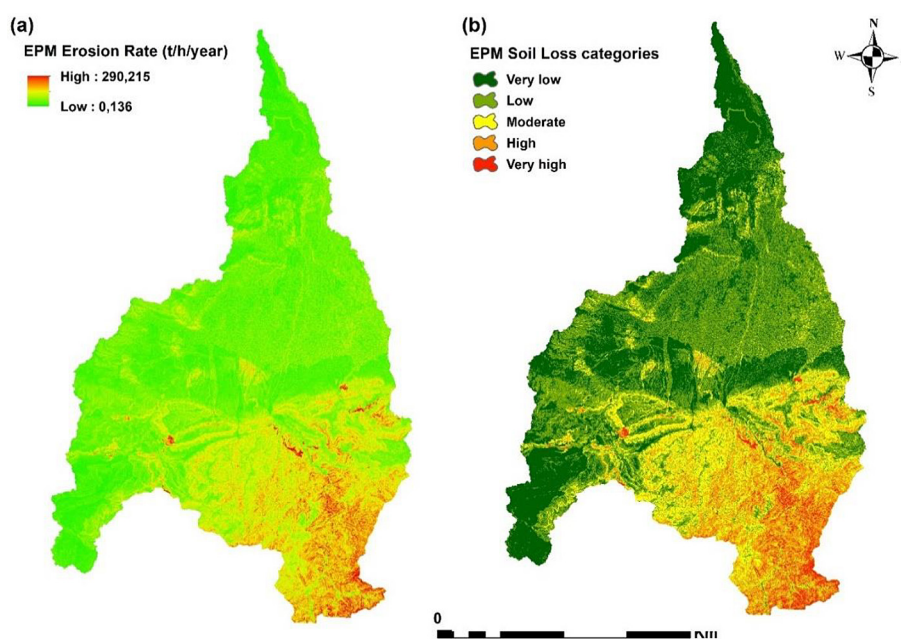


Figure 12. EPM map of land losse classes (t/h/year) in the Chichaoua watershed

erosion’s repercussions and impacts, we might therefore allocate regions with a large yearly output of sediment to regions with a significant probability of erosion. Conversely, to other areas where the yearly generation of sediment is still limited, erosion is essentially on the decline.

The influence of numerous man-made and natural factors that control the erosive dynamics causes the erosion rate to differ between the watershed’s several sections. Five classes are created from these units (Fig. 12b and Table 13) for the purpose of improving map readability, (16%) of the watershed area, which is situated in the south-west of the watershed close to the Boulaouane dam, is responsible for the high and extremely high land losses above 80 t/ha/year (Fig. 14d).

It suggests a slight spread of the phenomenon. The vast part among the research region (66%) is covered in the low to very low intensity class (less than 30 t/ha/year) (Fig. 13) that is concentrated in the basin’s north and south-central regions. Additionally, 18% of the entire area under investigation has losses ranging from 30 to 50 t/ha/year. Consequently, we can allocate regions with significant yearly sediment production to regions at high risk of erosion, which undoubtedly calls for better management to lessen the effects and repercussions of erosion. In contrast to other regions where the yearly generation of sediment is still limited, erosion is essentially on the decline.

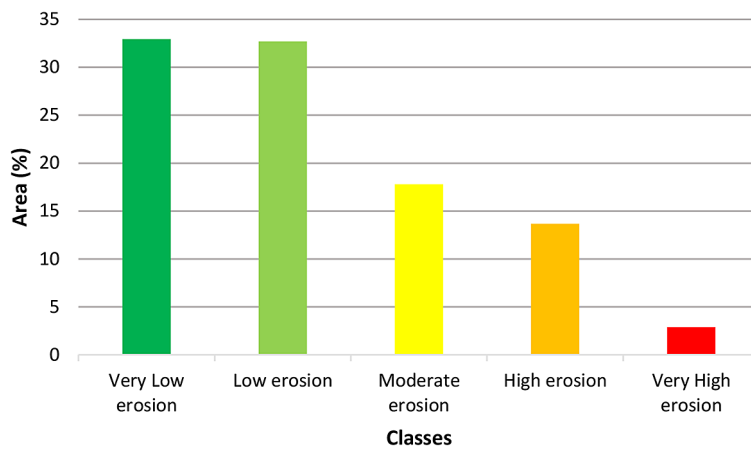


Figure 13. EPM Area classifications of the Chichaoua basin’s soil loss

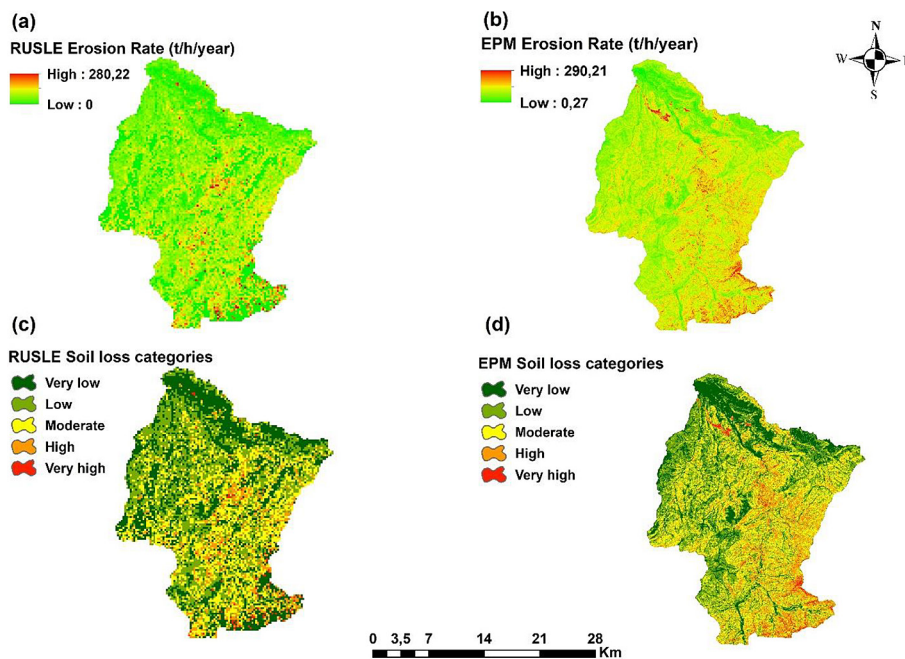


Figure 14. RUSLE and EPM maps of land loss classes (t/h/year) upstream the Boulaouane dam

Packaging rate and output of new dam sediment

The quantity of sediment actually released by the spilling watershed considered the sediment production (Vanoni, 1975). According to the most widely used calculation, the sedimentation ratio is the proportion of a basin’s annual soil loss to its sediment production.

Sediment yield divided by soil loss is the sediment delivery ratio (SDR) due to water erosion.

Many research has attempted to model this relationship with different factors: drainage density, land use, topography, while other researchers consider climate to be the dominant factor (Walling, 1996; Williams, 1977; Vanoni, 1975). Typically, these models are only applicable under the conditions in which they were developed.

This study is based on the formula of Hession and Shanholtz (1988), which is expressed by the following relationship:

$$SDR = 10 \times \left(\frac{R}{L}\right) \tag{16}$$

where: R – is the de-level among the plot and the exit; L – is the distance from the plot to the outlet.

With an area of 535.66 km², the SDR for the sub basin in our case above the Boulaouane dam is equivalent to 8%.

According to the findings, 92% of the sediments are locked in the long- and short-term traps that are located between the distribution line output and the field, and the remaining sediments are lodged in the exhaust.

For example, the quantity of sediment discharged into the exit is determined by the following ratio:

$$Ad = SDR \times A \tag{17}$$

where: A – the quantity of sediment generated at the slopes.

$$Ad = SDR \times Amoy = 8\% \times A \tag{18}$$

Lifetime dam

In Morocco, measures of solid transport in suspension or volume packed of reservoirs estimated via bathymetric profiles, ultrasonography surveys, or aerial photogrammetry have been specially used to provide a quantitative estimate of dam packaging. (Lahlou, 1994). In this research, we present a widely adopted method founded on the RUSLE and EPM models.

Given that the surface the sub-basin area above the dam is 567 km² and the average value of its specific degradation according to both the RUSLE and the EPM models are 32 t/ha/year and 55.43 t/he/year respectively. It can be deduced, that watershed’s contribution to the boiling of the Boulaouane watershed downstream are 1814400 t/year according to URSLE model and 3142881 t/year according to the EPM model respectively (Fig. 14a, Fig. 14b).

We will use the link that has been investigated between the packing rate and the specific degradation of the various dams at the Moroccan level in order to infer the lifetime of the dam in question. This correlation’s primary goal as shown in Figure 12 is to account for both the vase’s density and the volume of silt discharged from the dam (Table 2).

To estimate the lifespan of the future Boulaoune dam, currently under construction in the study area, it is essential to examine the relationship between the specific degradation

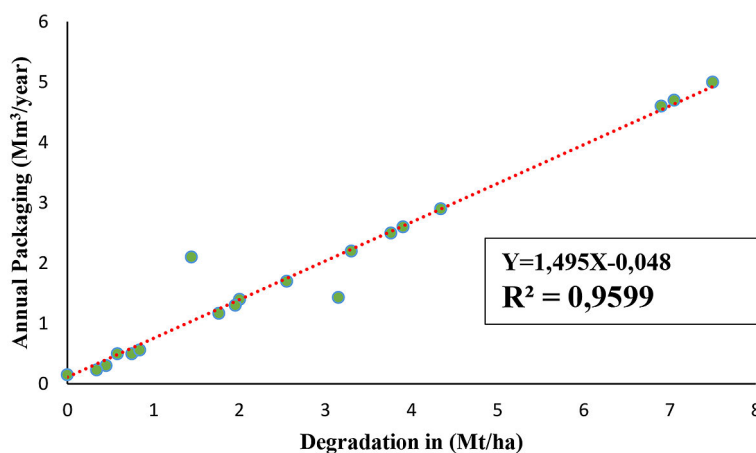


Figure 15. The relationship between specific degradations and the annual packaging of their respective dams (Table 2)

of various dams in Morocco and their siltation rates (data provided by the Hydraulic Basin Agency, Table 2). The calculation of the coefficient of determination ($R^2 = 0.9599$) indicates that 95.99% of the variance in the data is explained by the model, highlighting a strong linear correlation between watershed degradation and the annual siltation of dams (Fig. 15).

To verify the significance of this relationship, the correlation coefficient (R) was calculated as $R = \sqrt{R^2}$, yielding $R = 0.9797$. The t -statistic was then used to assess whether this correlation is significant. The formula applied is:

$$t = \frac{R\sqrt{n-2}}{\sqrt{1-R^2}} \quad (19)$$

where: $n = 20$ represents the number of data points. Substituting the values into the formula, we get:

$$t = \frac{0.9797 \cdot \sqrt{18}}{\sqrt{0.0401}} \approx 20.78 \quad (20)$$

Compared to the critical value ($t_{0.05,18} = 2.101$), this result confirms that the correlation is highly significant. The obtained regression equation is:

$$Y = 1.495X - 0.048 \quad (21)$$

where: Y – represents the watershed degradation (Mt/year), X – corresponds to the annual siltation rate (mm^3/year).

The regression coefficients ($\beta_1 = 1.495$ and $\beta_0 = -0.048$) were tested for their significance using t -tests. The results indicate that these coefficients are significantly different from zero at the

5% level, thereby validating the reliability of the regression equation (Montgomery et al., 2012).

To validate the significance of the coefficient of determination (R^2), the F -statistic was used according to the following formula:

$$F = \frac{R^2}{1-R^2} \times \frac{n-2}{1} \quad (22)$$

$$F = \frac{0.9599}{0.0401} \times 18 \approx 431.1 \quad (23)$$

This value significantly exceeds the critical value ($F_{0.05,1,18} = 4.41$), confirming that R^2 is highly significant (Kutner et al., 2004).

By applying this regression equation to the Chichaoua watershed, where the Boulaoune dam will be constructed, and considering the reservoir capacity (66 mm^3), it is possible to estimate its lifespan. The obtained results were compared with the bathymetric data of the Tasekourt dam, located in a neighboring watershed, to validate the estimation. This comparison supports the robustness of the predictions made.

In addition, by substituting the specific deterioration faced at the sub-basin level as it pours uphill from the Boulaouane dam, we will arrive at the following value:

2102261.57 m^3/year , or 2 mm^3/year according to model (EPM) 1213645.51 m^3/year , or 1 Mm^3/year according to Model (RUSLE)

With respect to the retention of the dam, which has a capacity of 66 million m^3 . The sheet erosion contributes annually to 1.55% of the dam’s packaging, giving it a lifespan of 54 years. According to the RUSLE model, and 3% of the tank packaging, or 33 years, according to the EPM model,

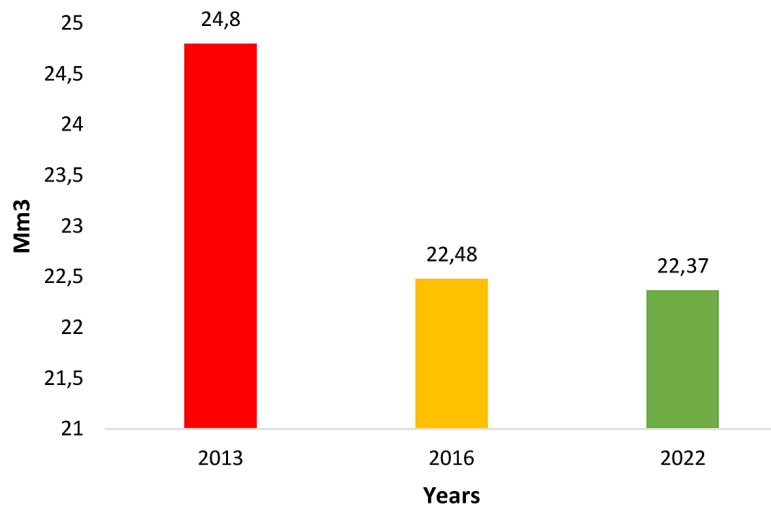


Figure 16. Development of the typical capability of the Taskourt dam

which leaves out the other sources of sediment (linear, mass, and hydrographic erosion).

The validity of the models utilised

In comparison to the RUSLE approach, which yields results that are comparatively more accurate, the EPM method slightly overestimates the outcomes. On both time scales, the two models operated quite similarly. Additionally, the RUSLE model tends to depict the results of comparable erosion rates found by the most recent bathymetric measurements in the watering basin of the nearby Taskourt dam at the level of the Assif El Mal watering subbasin (0.8 mm³/year), according to the ABHT (Tensift Hydraulic Basin Agency) (Fig. 16). However, the RUSLE model often predicts the actual outcomes.

DISCUSSION

In the Chichaoua basin, simultaneous reading of soil loss assessment maps reveals a fluctuating erosion classes' distribution, highlighting the total amount effect of the various water erosion contributing factors. Results of the study show that even on steep slopes, the presence of abundant vegetation (forest) considerably lowers erosion rates. However, regions with medium to high slopes and no vegetation are more vulnerable to erosion. The topography of the study region may also have an impact on the water erosion phenomenon, in addition to the plant cover. It has been noted that regions with medium to high erosion risk typically observe the slope and altitude dispersion on the map; that is, they focus on regions with medium to strong slope and altitude.

According to the RUSLE model, a very low danger of erosion exists in 73.36% of the watershed area, 13.4% a minimal danger, 8.02% a mild danger, 0.56% is a severe type danger, while 4.65% is a high danger (Fig. 9). The range of annual land losses is 0–280.22 t/ha. 10.03 t/ha/year was the average loss.

Results from the EPM model indicate that 32.94% of the watershed area has an extremely minimal erosion risk, 32.7% a low risk, 17.80% a moderate danger, 13.67% a significant danger and 2.88% a danger of severe type (Fig.12). Annual losses of land varies from 0.136 to 290.21 t/ha/year. It was 27.53 t/ha/year on average.

These values correspond to a medium low risk of erosion, as a global status for the entire

watershed. Indeed, this average remains lower than those found in other areas in Morocco where water erosion is intense.

The watershed of Kalaya and Oued Sania, in the northwestern Rif, have averaged erosion rates of 47.18 t/hour/year (Tahiri et al., 2014, 2017) and 34.74 t/h/year (Khali et al., 2016), respectively.

Land losses in the Oued Salha (Central Rife) and Oued Boussouab (Eastern Rife) basins were approximately 55.53 tonnes per hectare per year (Sadiki et al. 2004) and 22 tonnes/hour/year, respectively (Sadiki and al., 2009). The Sebou Basin, which covers more than 70% of the Gharb region, has an annual growth of 10 t/h (Chadli, 2016). According to the authors, the Oum Er-Rbia basin in the Middle Atlas has fluctuating rates between 58 t/h/year (El Jazouli et al., 2019) to 224 t/hour/year (Yjjou et al., 2014). Finally, in the N'fis basin in the Western Upper Atlas, it is approximated that there is an erosion of 115 t/h/year (Markhi et al., 2015).

Based on our study, when comparing the maximum erosion rates in the Chichaoua basin, calculated using the RUSLE and EPM methods, reaching 280 t/h/year and 290 t/h/year, respectively, it is clear that these values remain relatively low compared to those observed in the N'fis (Markhi et al., 2015), and the Ourika basin of two basins of the Upper Atlas of Marrakech. Soil losses are lower than 1500 t/h/year in the N'fis watershed, while they are greater than 2000 t/h/year in the Ourika watershed.

This characteristic classifies the Chichaoua watercourse as low erosion basin. The reason for this is that surface areas and rainfall erosion factors are more significant in the Ourika and N'fis basin than in the Chichaoua basin. In the Ourika basin, the erosive precipitation is 100 MJ mm/ha.h.a, while in the N'fis basin, it is 57 MJ mm/h.a. and an upper limit of 116 MJ/ha.h.a in the Chichaoua watering basin. The topographic dimension is also greater in the spilling basin of the Ourika and N'fis than in that of Chichaoua.

Therefore, although the three sloping basins are in the same High-Atlantic context, the climatic and topographic factors vary slightly, which could account for the discrepancies noted in the susceptibility of the three basins to water erosion.

However, the amount of sediment transported, which is estimated at 1 and 2 million tonnes per year according to the two models, RUSLE and EPM, respectively, from the subbasin above

the dam, poses a real challenge for the filling of the Boulaouane dam.

A SIG that incorporates the model presents numerous advantages. It enables efficient handling of substantial data regarding different aspects of water erosion. Additionally, it enables visualization of soil loss or potential erosion rates (t/ha/year) along with the geographical dispersion of vulnerability to erosion throughout different regions of the spill catchment. It is crucial to highlight that the universal equation for soil loss solely considers average losses from soil loss.

Applying the model under different circumstances and on a larger scale than those for which it was originally developed raises concerns about its precision, as it relies on incomplete data or very limited spill basins. Furthermore, the model assumes that there is erosion on all surfaces if any factors are not zero and fails to indicate where deposits are located.

Nonetheless, uncertainty can be accepted provided that field measurements and laboratory analyses are conducted meticulously (Renard et al., 1997).

Therefore, although the reliability of the results obtained is questionable, the methodology enables managers and policymakers to anticipate measures to prevent erosion in regions that are at high risk of erosion. It also explains how soils can be used by arrangements to combat erosion phenomena.

The EPM approach has not yet been used in Moroccan territory. Nevertheless, it would be interesting to compare and discuss the results achieved in the Chichaoua basin combining the EPM model with other Moroccan-standard concepts and techniques.

A quantitative model that is suggested for semi-arid mountain environments is the EPM model, despite the fact that each model has advantages and disadvantages (Rajabi et al., 2022). This model is unique in that it incorporates a number of factors into the estimation of soil loss (W), taking into account each pixel's erosive condition, lithology, NDVI, precipitation, slope, soil temperature, and land use (Ansar et al., 2020). Additionally, the EPM model makes it possible to calculate a variety of erosion types, such as gully-erosion, landslides, and sheet erosion.

The EPM uses a multiplicative method to calculate erosion, and under GIS, it attempts to categorize the data into qualitative groups rather than extrapolating, which raises errors and uncertainties. Furthermore, there is ambiguity around

the kind of interpolation along with The weather stations' limited number that were utilized in the calculation of the climatic erosivity factor (Oualali et al., 2020).

There are a few internal and exterior limitations with this model, though. The model's assumption for data management via GIS is that each 25-meter resolution cell's topography, soil utilization variables, erosion, and erosion are all the same (Ouallali et al., 2020).

The impacts of sudden changes in crop types and cover from one season to the next are not included by the EPM model. Specifically, it ignores the fact that grass coverage decreases erosion in the summer and loses its effectiveness in the fall, as demonstrated by (Biddoccu et al., 2016) in other areas with climates distinct from the Chichaoua basin.

However, the EPM model cannot provide an exact land loss quantity, it can highlight geographical disparities in erosion (Hoyos, 2005). The spatial analysis of the sedimentary production potential shows that the majority of sediments present in the upward zone of the future Boulaoune dam are located in a very hard terrain (very strong water erosion), which facilitates their transportation to the retention of the dam.

However, when the area was cultivated or devoid of vegetation, topographical erosion is exacerbated and hastened, particularly during wet seasons. Moreover, the primary determinants of rate of erosion were length of the slope and slope, with the exception of regions where water collects (such as ravines and streams).

Compared to the RUSLE methodology, which produced results that were comparatively more accurate, the EPM method slightly exaggerated the outcomes. On both time scales, the two models' performances were quite comparable. Furthermore, EPM's model overestimates findings, while the RUSLE model more closely approximates the mean annual sediment discharge and yield values that are "actual" (measured). Overall, the two methods accurately depicted the phenomenon, allowing for the discovery of the region's most susceptible to erosion.

Findings from this modeling of water erosion, albeit providing only imprecise and approximative values, have the potential to assist local actors in their decision-making with respect to resource management and soil preservation. By utilizing a variety of scenarios to determine and confirm the best anti-erosion management method, the GIS has made the simulation possible and

feasible today. Results from a threefold comparison regional, factor, and methodological could be obtained for comparative analysis. To build a coordinated response to erosion, we want to gain an understanding of the regional pattern of land losses at the Western High Atlas level by contrasting the results of water erosion research conducted in the Chichaoua basin and Morocco.

To verify the accuracy of the results estimated by both methods (280 and 290 t/ha/year), we should not stop at this point. Regarding advantages and limitations of every technique, it is clear that this disparity in the results of the two methods is justified because RUSLE only gives the rates of erosion at the level of the surface (bottle erosion), while EPM gives the overall erosion rate (result of the different forms of the erosion).

This work stands out for its innovative approach in assessing and predicting soil loss from water erosion in a region where a dam is being built in the future. By combining two quantitative methods, namely the RUSLE and EPM models, this study provides a thorough and comparative analysis of potential soil losses. These approaches allow possible to precisely quantify the effects of several factors, such as vegetation cover, land use, and slope on erosion processes. These findings provide a robust scientific basis to guide policymakers on soil conservation strategies and land management is essential to sustaining natural resource management in preparation for the future dam construction.

CONCLUSIONS

The study concludes by highlighting the significance of water sedimentation and erosion, emphasizing the need for thorough evaluation and understanding to mitigate their adverse effects. Utilizing GIS alongside empirical models has facilitated large-scale spatialization of erosion, enabling the determination of regions that need urgent action to preserve soil. Utilizing the EPM and RUSLE models in the Chichaoua basin has revealed the erosion risk's spatial distribution, with key factors such as lithology and vegetation cover influencing erosion intensity. The study quantifies soil loss using both RUSLE and EPM models, indicating variations in estimated sediment output and dam lifespan. Sediment inputs from tributaries play a crucial role in dam packing, predominantly attributed to padded erosion. Furthermore, the study suggests planning

initiatives for soil conservation and dam lifespan extension based on its findings and maps. The need for continued investigation into degradation factors, including local resources and human activities, is emphasized. Both Rusle and EPM approaches offer valuable insights at the watershed level, with RUSLE focusing on pad erosion and EPM highlighting priority intervention areas and total degradation caused by various erosion types.

Ultimately, the recommendation to apply the EPM technique to the entire basin for practicality underscores the study's commitment to providing actionable insights for sustainable land and water management practices. Dump erosion is thought to be the primary cause of the dam packaging phenomena, and the RUSLE model is most appropriate for the sub-basin flowing upwards of the planned Boulaouane dam.

Acknowledgments

The authors express their sincere gratitude to the researchers supporting the PRIMA Resilink project for their invaluable support of this research article. In addition, they sincerely appreciate the anonymous reviewers for their insightful and constructive comments.

REFERENCES

1. ABHT, (2013). Presentation of the Tensift Hydraulic Region, Internal Report, 20.
2. ABHT, (2015). Monitoring of water quality in the Tensift basin.
3. Ait Fora A. (1995). Spatial modeling of water erosion in a basin of the Moroccan Rif: validation of the geomatic approach by sedimentology, radioactive tracers and magnetic susceptibility of sediments. PhD Thesis, University of Sherbrooke, Quebec, 231.
4. Al-Mamari, M. M., Kantoush, S. A., Al-Harrasi, T. M., Al-Maktoumi, A., Abdrabo, K. I., Saber, M., & Sumi, T. (2023). Assessment of sediment yield and deposition in a dry reservoir using field observations, RUSLE and remote sensing: Wadi Assarin, Oman. *Journal of Hydrology*, 617, 128982.
5. Ansar, A., & Azaiez, N. (2020). Qualitative and quantitative aspects of climate change in Ghardaia (Algeria). *Human Sciences Journal*, 549–565.
6. Argaz A., Darkaoui A. & Bikhtar H., and al. 2019. Using EPM Model and GIS for Estimation of Soil Erosion in Souss Basin, Morocco. *Turkish Journal of Agriculture-Food Science and Technology*, 7(8), 1228–1232.

7. Arnold J.G., Srinivasan R., Muttiah R.S. et al. (1998). Large area hydrologic modeling and assessment part I: Model development. *Journal of American Water Resources Association*, 34, 73–89.
8. Baiddah, A., Krimissa, S., Hajji, S., Ismaili, M., Abdelrahman, K., El Bouzekraoui, M.,... & Namous, M. (2023). Head-cut gully erosion susceptibility mapping in semi-arid region using machine learning methods: insight from the high atlas, Morocco. *Frontiers in Earth Science*, 11, 1184038.
9. Badraoui, A., & Hajji, A. (2001). Envasement des retenues de barrages. *La Houille Blanche*, 87(6–7), 72–75. Benmansour M., Ibn Majah M., Marah H., et al. (2000). *Use of the 137 Cs technique in soil erosion in Morocco – Case study of the Zitouna basin in the north*. Proceeding of an international Symposium on Nuclear Techniques in Integrated Plant Nutrients, Water and Soil management, IAEA/FAO, 308–315.
10. Biddoccu, M., Ferraris, S., Opsi, F., & Cavallo, E. (2016). Long-term monitoring of soil management effects on runoff and soil erosion in sloping vineyards in Alto Monferrato (North–West Italy). *Soil and Tillage Research*, 155, 176–189.
11. Borrelli P., Robinson D.A., Fleischer L.R., et al. (2017). An assessment of the global impact of 21st century land use change on soil erosion. *Nature Communications*, 8(1), 2013.
12. Bouamrane, A., Bouamrane, A., & Abida, H. (2021). Water erosion hazard distribution under a Semi-arid climate Condition: Case of Mellah Watershed, North-eastern Algeria. *Geoderma*, 403, 115381.
13. Bouhlassa S. & Bouhsane N. (2019). Assessment of areal water and tillage erosion using magnetic susceptibility: the approach and its application in Moroccan watershed. *Environmental Science and Pollution Research*, 1–15.
14. Bouhlassa S., Moukhchane M. & Aiachi A. (2000). Estimate of soil erosion and deposition of cultivated soil of Nakhla watershed, Morocco, using 137 Cs technique and calibration models. *Acta Geologica Hispanica*, 35(3/4), 239–249.
15. Bou-Imajjane, L., Belfoul, M. A., Elkadiri, R., & Stokes, M. (2020). Soil erosion assessment in a semi-arid environment: a case study from the Argana Corridor, Morocco. *Environmental Earth Sciences*, 79, 1–14.
16. Brown, R.B. (2003). *Soil Texture, Soil and Water Science Department, Florida Cooperative Extension Service, Institute of Food and Agricultural Sciences, University of Florida, Fact Sheet SL29*, 8.
17. Bunzl K. & Kracke W. (1988). Cumulative deposition of 137Cs, 238Pu, 239+240 Pu and 241Am from global fallout in soils from forest, grassland and arable land in Bavaria. *Journal of Environmental Radioactivity*, 8(1), 1–14.
18. Chaaouan, J., Faleh, A., Sadiki, A., Mesrar, H. (2013). Télédétection, SIG et modélisation de l'érosion hydrique dans le bassin versant de l'oued Amzaz, Rif Central. *Revue Française de Photogrammétrie et de Télédétection*, 203, 19–25. <https://doi.org/10.52638/rfpt.2013.26>
19. Chadli, K. (2016). Estimation of soil loss using RUSLE model for Sebou watershed (Morocco). *Modeling Earth Systems and Environment*, 2, 1–10.
20. Damnati B., Chatt A, Hamani M., et al. (2006). The water erosion and its quantification by the radio element 137Cs at the level of the watershed of the Raouz dam (TangerTétouan Region). TANCA-01. Workshop on analytical, nuclear and conventional techniques and their applications. Rabat 8–9 December, 38.
21. Damnati B., Ibrahim S., Benhardouze O., et al. (2010). Quantification of erosion by excess 137Cs and 210Pb: case of a plot at the basin level of the Nakhla dam (Tetouan Region, Northwestern Morocco). *Africa Geoscience Review*, 17(3), 215–223.
22. Durigon, V. L., Carvalho, D. F., Antunes, M. A. H., Oliveira, P. T. S., & Fernandes, M. M. (2014). NDVI time series for monitoring RUSLE cover management factor in a tropical watershed. *International journal of remote sensing*, 35(2), 441–453.
23. El Garouani A., Tribak A. & Abahrour M. (2010). Assessment the effects of land-use cover changes on regional soil loss susceptibility using RUSLE model and remote sensing data. Red Books. *International Association of Hydrological Sciences Publication*, 340, 343–349.
24. El Hafid, D., Zerrouqi, Z., & Akdim, B. (2017). Étude des séquences de sécheresse dans le bassin d'Isly (Maroc oriental). *Larhyss Journal*, 31, 83–94.
25. El Jazouli A., Barakat A., Khellouk R. and al. 2019. Remote sensing and GIS techniques for prediction of land use land cover change effects on soil erosion in the high basin of the Oum ErRbia River (Morocco). *Remote Sensing Applications. Society and Environment*, 13, 361–374.
26. El Mouatassime S., Boukdir A., Karaoui I. et al. 2019. Modelling of soil erosion processes and runoff for sustainable watershed management: case study oued el Abid watershed, Morocco. *Agriculture & Forestry*, 65(4), 241–250.
27. Elaloui A., Marrakchi C., Fekri A., et al. 2017. USLE-based assessment of soil erosion by water in the watershed upstream Tessaoute (Central High Atlas, Morocco). *Modeling Earth Systems and Environment*, 3(3), 873–885.
28. Elbukaou, K., Ezzine, H., Badrahou, M., Rouchdi, M. and Ozer, A. (2005). Remote detection and GIS methodological approach to the evaluation of the potential risk of water erosion in the Oued Srou Basin (Moyen Atlas, Morocco), *Geo-Eco-Trop*, 29, 25–36.

29. Ezzaouini M.A., Mahé G., Kacimi I. et al. (2020). Comparison of the MUSLE Model and Two Years of Solid Transport Measurement, in the Bouregreg Basin, and Impact on the Sedimentation in the Sidi Mohamed Ben Abdellah Reservoir, Morocco. *Water*, 12, 1882.
30. Faleh A. & Maktite A. (2014). Map of areas vulnerable to water erosion using the PAP/CAR method and GIS above Allal el fassi dam, medium Atlas (Maroc). *Papeles de Geografía*, (59–60), 71–82.
31. Fathallah, F.E., Algouti, A., & Algouti, A. (2021). Normalized difference vegetation index (NDVI) of the Chichaoua Watershed-Morocco: Comparison and evolution. *Journal of Analytical Sciences and Applied Biotechnology*, 3(1), Anal-Sci.
32. Flanagan D.C. & Nearing M.A. (1995). USDA Water Erosion Prediction Project hillslope and watershed model documentation. *Nserl Rep*, 10, 1–123.
33. Ganasri, B.P., & Dwarakish, G.S. (2015). Study of land use/land cover dynamics through classification algorithms for Harangi catchment area, Karnataka State, India. *Aquatic Procedia*, 4, 1413–1420.
34. Gavrilović, S. (1972). Engineering of torrents and erosion. *Journal of Construction* (Special Issue), Belgrade, Yugoslavia.
35. Gavrilovic S. (1966). *Methodology for Classification of Erosion Processes and Mapping of Eroded Areas*. Stage I, Beograd, Institute Jaroslav Černi.
36. Gavrilovic, S. (1962). *A method for estimating of the average annual quantity of sediments according to the potency of erosion*. Bull. Fac. For, 26, 151–168.
37. Gavrilovic, S. (1970). *Modern ways of calculating the torrential sediment and erosion mapping*. Erosion, Torrents and Alluvial Deposits; Yugoslav Committee for International Hydrological Decade: Belgrade, Serbia, 85–100.
38. Gavrilovic, Z. (1988). Use of an empirical method (Erosion Potential Method) for calculating sediment production and transportation in unstudied or torrential streams. In *International Conference on River Regime*; Hydraulics Research Ltd.: Wallingford, UK, 411–422.
39. Hadri, A., Saidi, M.E.M., Saouabe, T., & El Alaoui El Fels, A. (2021). Temporal trends in extreme temperature and precipitation events in an arid area: case of Chichaoua Mejjate region (Morocco). *Journal of Water and Climate Change*, 12(3), 895–915. Abdessamad Hadri, Mohamed El Mehdi Saidi, Tarik Saouabeand Abdelhafid El Alaoui El Fels
40. Hembram, T.K., Paul, G.C., & Saha, S. (2019). Comparative analysis between morphometry and geo-environmental factor based soil erosion risk assessment using weight of evidence model: a study on Jainti river basin, eastern India. *Environmental processes*, 6(4), 883–913.
41. Hession, W.C., & Shanholtz, V.O. (1988). A geographic information system for targeting non-point-source agricultural pollution. *Journal of Soil and Water conservation*, 43(3), 264–266.
42. Hoyos, N. (2005). Spatial modeling of soil erosion potential in a tropical watershed of the Colombian Andes. *Catena*, 63(1), 85–108.
43. Hssaine, A.A. (2014). Elements on the hydrology of the Atlantic part of the Oud Guir (South-Eastern Morocco) and on the catastrophic flood of 10 October 2008. *Physio-Geo. Physical Geography and Environment*, 8, 337–354.
44. Ibrahim, S. (2005). *Application of 210Pbex as an alternative to the use of 137Cs for the study of soil redistribution on cultivated and uncultivated transects, El Hachef and Raouz Basins, northern Morocco*, PhD Thesis in Sciences, Abdelmalek Essaadi University, Tangier, Morocco.
45. Issa, L.K., Lech-Hab, K.B.H., Raissouni, A., & El Arrim, A. (2016). Quantitative mapping of soil erosion risk by SIG/USLE approach at Kalaya basin level (Maroc Nord Occidental). *J Mater Environ Sci*, 7(8), 2778–2795.
46. Jain, M.K., & Das, D. (2010). Estimation of sediment yield and areas of soil erosion and deposition for watershed prioritization using GIS and remote sensing. *Water Resources Management*, 24(10), 2091–2112.
47. KhaliIssa L., Lech-Hab KBH., Raissouni A., et al. (2016). Quantitative mapping of soil erosion risk by SIG/USLE approach at Kalaya Basin Level (Maroc Nord Occidental). *Journal of Materials and Environmental Science*, 7(8), 2778–2795.
48. Kutner, M.H., Nachtsheim, C.J. & Neter, J. (2004). *Applied Linear Regression Models*, Fourth edition. McGraw-Hill Irwin, Boston.
49. Lahlou, A. (1994). Envasement des barrages au Maroc. Wallada. Lammadalena N. 2010. Climate change and water resources in the Mediterranean region. *The Watchtower of CIHEAM*, 12, 1–4.
50. Lazarevic R. (1985). *The new method for erosion coefficient determination – Z. Erosion - professional factsheet*, 13; 54–61. (In Serbian).
51. Lazarevic, R. (1968). Erosion in the Gvozdacka river basin –supplement to the instructions for erosion map elaboration. *Bulletin of the Serbian Geographical Society*, 49(2), 75–98. (In Serbian).
52. Mandimou, S. (2002). Modelling and mapping of water erosion for the integrated layout of the Moulay Bouchta River Basin (Rif occidental). 3rd cycle memory, ENFI, Salé, 105(3)
53. Markhi A., Laftouhi N., Grusson Y., et al. (2019). Assessment of potential soil erosion and sediment yield in the semi-arid N' fis basin (High Atlas, Morocco) using the SWAT model. *Acta Geophysica*, 67(1), 263–272.

54. Markhi A., Laftouhi N., Soulaïmani A., Fniguire F. (2015). Quantification and evaluation of water erosion using the RUSLE model and reporting integrated into a GIS. Application in the watering basin in the high atlas of Marrakech (Maroc). *European Scientific Journal* October 2015 edition 11(29).
55. Meliho, M., Khattabi, A., Zine El Abidine, A. (2016). Study of water erosion sensitivity in the Urika basin (Haut Atlas, Maroc). *First AMRS Congress and 23rd APDR Congress 'Sustainability of Territories in the Context of Global Changes*, 189–196.
56. Mohammed, S., Abdo, H. G., Szabo, S., Pham, Q. B., Holb, I. J., Linh, N. T. T.,... & Rodrigo-Comino, J. (2020). Estimating human impacts on soil erosion considering different hillslope inclinations and land uses in the coastal region of Syria. *Water*, 12(10), 2786.
- Montgomery, D. R. (2012). *Dirt: The Erosion of Civilizations*, with a New Preface. Univ of California press.
57. Moore, I. D., & Wilson, J. P. (1992). Length-slope factors for the Revised Universal Soil Loss Equation: Simplified method of estimation. *Journal of soil and water conservation*, 47(5), 423–428.
58. Mosaid, H., Barakat, A., Bustillo, V., & Rais, J. (2022). Modeling and mapping of soil water erosion risks in the Srou Basin (Middle Atlas, Morocco) using the EPM model, GIS and magnetic susceptibility. *Journal of Landscape Ecology*, 15(1), 126–147.
59. Ouallali, A., Aassoumi, H., Moukhchane, M., Moumou, A., Houssni, M., Spalevic, V., & Keesstra, S. (2020). Sediment mobilization study on Cretaceous, Tertiary and Quaternary lithological formations of an external Rif catchment, Morocco. *Hydrological Sciences Journal*, 65(9), 1568–1582.
60. Pandey A., Mathur A., Mishra S.K. et al. (2009). Soil erosion modeling of a Himalayan watershed using RS and GIS. *Environmental Earth Sciences*, 59(2), 399–410.
61. Paroissien J.B., Darboux F., Couturier A. et al. (2015). A method for modeling the effects of climate and land use changes on erosion and sustainability of soils in a Mediterranean watershed (Languedoc, France). *Journal of Environmental Management*, 150, 57–68.
62. PDAIRE.ABHT). -ABHT, (1995). *The objectives of establishing hydraulic basin agencies*. Internal report, 39.
63. Rahhou M., (1999). *Erosion in the Central Prefecture, interfluvial zone Leben-Sebou-Ouerga, a continuation of natural evolution, a social production*. State Doctoral Thesis, Mohammed V University, Rabat, 300.
64. Rajabi, A.M., Yavari, A., & Cheshomi, A. (2022). Sediment yield and soil erosion assessment by using empirical models for Shazand watershed, a semi-arid area in center of Iran. *Natural Hazards*, 112(2), 1685–1704.
65. Rawls, W.J., & Brakensiek, D.L. (1982). Estimating soil water retention from soil properties. *Journal of the Irrigation and Drainage Division*, 108(2), 166–171.
66. Remini B., Leduc C. & Hallouche W. (2009). Évolution des grands barrages en régions arides : quelques exemples algériens. *Sécheresse*, 20(1), 96–105.
67. Renard K.G., Foster G.R., Weesies G.A. et al. (1991). RUSLE: Revised Universal Soil Loss Equation. *Journal of soil and water conservation*, 46, 30–33.
68. Renard K.G., Foster G.R., Weesies G.A., McCool D.K., Yorder D.C., (1996). *Predicating soil loss equation (RUSLE)*. USDA/ARS. ARG. AG. Handbook # 703. Washington. DC.
69. Renard, K.G., & Freimund, J.R. (1994). Using monthly precipitation data to estimate the R-factor in the revised USLE. *Journal of hydrology*, 157(1–4), 287–306.
70. Renard, K.G., Foster, G.R., Weessies, G.A., McCool, D.K., Yoder, D.C. (eds). (1997). *Predicting Soil Erosion by Water: A guide to conservation planning with the Revised Universal Soil Loss Equation (RUSLE)*. U.S. Department of Agriculture, Agriculture Handbook 703.
71. RESING AHT GROUP AG Date: November 2016 Final diagnosis of the Chichaoua subbasin).
72. Ritchie J.C. & Machenry J.R. (1990). Application of radioactive fallout cesium-137 for measuring soil erosion and sediment accumulation rates and patterns. *Journal of Environmental Quality*, 19, 215–233.
73. Roose E. (1994). Introduction to the conservation management of water, biomass and soil fertility (GCES) FAO Pediatric Bulletin. 70, 420.
74. Roose, E.J. and Lelong, F. (1976). The factors of water erosion in tropical Africa study on small experimental plots of soil. *Journal of Physical Geography and Dynamic Geology*, XVIII(4), 365–374.
75. Rouichi H. (1996). *Erosion processes and factors in the Bouregreg basin (s.s) sedimentological approach to the quantification of erosion*. Doctoral thesis, Mohamed V University, Rabat.
76. Sabir, M., Roose, E., Machouri N., & Nouri, A. (2002). Rural management of natural resources in two terroirs of the Mediterranean mountains of the Western Rif. *Bulletin of the network erosion, IRD, Montpellier*, 21, 456–471.
77. Sadiki A., Faleh A., Navas A. et al. (2007). Assessing soil erosion and control factors by the radiometric technique in the Boussouab catchment, Eastern Rif, Morocco. *Catena*, 71(1), 13–20.
78. Sadiki, A., Bouhlassa, S., Auajjar, J., Faleh, A., & Macaire, J.J. (2004). Utilisation d'un SIG pour l'évaluation et la cartographie des risques d'érosion par l'Equation universelle des pertes en sol dans le Rif oriental (Maroc): cas du bassin versant de l'oued Boussouab. *Bulletin de l'Institut Scientifique, Rabat, section Sciences de la Terre*, 26(2004), 69–79.
79. Sadiki, A., Faleh, A. Zêzere, J. L., & Mastass, H.

- (2009). Quantification of Erosion in Nappes in the Upper Basin of the Oued Sahla-Rif Central Morocco. *Geographic Specifications*, 6, 59–70.
80. Salma, K., Ahmed, A., Abdellah, A., & Akram, E.G. (2023). Quantification of water erosion using empirical models RUSLE and EPM in the Rheraya basin in the High Atlas of Marrakech. *Disaster Advances*, 16(5), 19–28.
 81. Shin G.J. (1999). Department of Civil Engineering, Gang-won National University, Ph.D. dissertation, The study of soil erosion analysis in watershed using GIS.
 82. Shin, S. S., Park, S. D., Cho, J. W., & Lee, K. S. (2008). Effects of vegetation recovery for surface runoff and soil erosion in burned mountains, Yangyang. *KSCE Journal of Civil and Environmental Engineering Research*, 28(4B), 393–403.
 83. Stone, R.P. and Hillborn D. (2000). *Universal Soil Loss Equation, Ontario, Canada*, Ontario Ministry of Agriculture and Food (OMAFRA).
 84. Tahiri M., Tabyaoui H., El Hammichi F., et al. (2014). Evaluation and quantification of erosion and sedimentation based on the RUSLE, MUSLE and integrated GIS deposition models. Application to the Oued Sania Basin (Bassin de Tahaddart, Rif nord occidental, Maroc). *European Journal of Scientific Research*, 125(2), 157–178.
 85. Tahiri, M., Tabyaoui, H., El Hammichi, F., Achab, M., Tahiri, A., & El Hadi, H. (2017). Quantification de l'érosion hydrique et de la sédimentation à partir de modèles empiriques dans le bassin versant de Tahaddart (Rif nord occidental, Maroc). *Bulletin de l'Institut Scientifique, Rabat, Section Sciences de la Terre*, 39, 87–101.
 86. Thompson R., Stober J.C., Turner G J. et al. (1980). Environmental applications of magnetic measurements. *Science*, 207, 481–486.
 87. Vanoni, V.A. (1975). River dynamics. *Advances in applied mechanics*, 15, 1–87.
 88. Walling, D.E., & Webb, B.W. (1996). Erosion and sediment yield: a global overview. *IAHS Publications-Series of Proceedings and Reports-Intern Assoc Hydrological Sciences*, 236, 3–20.
 89. Williams, J.R. (1977). *Sediment delivery ratios determined with sediment and runoff models*.
 90. Wischmeier V.H. & Smith D.D. (1978). *Predicting rainfall erosion losses: A guide to conservation planning*. United States Department of Agriculture in cooperation with Purdue Agricultural Experiment Station. United States Department of Agriculture, Washington. Agriculture Handbook 282.
 91. Wischmeier W.H and Smith, D.D. (1981). *Predicting rainfall erosion losses. a guide to conservation planning*. Supplement to Agriculture Handbook No. 537, USDA, Washington. 58.
 92. Wischmeier, W.H., Smith, D.D., and Uhland R.E. (1958). Evaluation of factors in the soil-loss equation. *Agricultural Engineering* 39, 458–462.
 93. Xinbao Z., Walling D.E., Mingy F., et al. (2003). 210Pbex depth distribution in soil and calibration models for assessment of soil erosion rates from 210Pbex measurements. *Chinese Journal*, 48(8), 813–818.
 94. Yjjou M., Bouabid R., El Hmaidi A et al. (2014). Modeling of water erosion via GIS and the universal soil loss equation at the level of the Oum Er-Rbia watercourse. *The International Journal of Engineering and Science (IJES)*, 3(8) 83–91.
 95. Yjjou, M., Bouabid, R., El Hmaidi, A., and Es-sahlaoui, A. (2012). Topographic and climate characterization via GIS of the Oum Er-Rbia basin above the El Hansali dam (Middle Atlas SW, Morocco), *Journal of Hydrocarbons Mines and Environmental Research*, 3(2), 104–109.
 96. Zahnoun, A.A., Makhchane, M., Chakir, M., Al Karkouri, J., & Watfae, A. (2019). Estimation and cartography the water erosion by integration of the Gavrilovic “EPM” model using a GIS in the Mediterranean watershed: Lower Oued Kert watershed (Eastern Rif, Morocco). *International Journal of Advance Research, Ideas and Innovations in Technology*, 5(6), 367–374.
 97. Zahnoun, A.A., Makhchane, M., Chakir, M., Al Karkouri, J., & Watfae, A. (2019). Estimation and cartography the water erosion by integration of the Gavrilovic “EPM” model using a GIS in the Mediterranean watershed: Lower Oued Kert watershed (Eastern Rif, Morocco). *International Journal of Advance Research, Ideas and Innovations in Technology*, 5, 367–374.
 98. Zhang X.C. (2017). Evaluating water erosion prediction project model using cesium-137-derived spatial soil redistribution data. *Soil Science Society of America Journal*, 179–188.
 99. Zhang Y., Zhang Z., Xue S., Wang R., Xiao M. (2020). Stability analysis of a typical landslide mass in the Three Gorges Reservoir under varying reservoir water levels. *Environmental Earth Sciences*, 79, 1–14.
 100. Zouagui A. (2010). Application of isotopic techniques (137Cs) to the estimation of water erosion in the watershed of My Bouchta, Western Rif, Morocco. 3rd cycle memory, *ENFI*, 81.